Fault Tolerant Control for Bimodal Piecewise Affine Systems

Nastaran Nayebpanah

A Thesis

in

The Department

of

Mechanical and Industrial Engineering

Presented in Partial Fulfillment of the Requirements

for the Degree of Master of Applied Science (Mechanical Engineering) at

Concordia University

Montréal, Québec, Canada

January 2010

© Nastaran Nayebpanah, 2010

Library and Archives Canada

Published Heritage Branch

395 Wellington Street
Ottawa ON K1A 0N4
Canada

Bibliothèque et Archives Canada

Direction du Patrimoine de l'édition

395, rue Wellington
Ottawa ON K1A 0N4
Canada

Your file Votre référence
ISBN: 978-0-494-67315-7
Our file Notre référence
ISBN: 978-0-494-67315-7

NOTICE:

The author has granted a non-exclusive license allowing Library and Archives Canada to reproduce, publish, archive, preserve, conserve, communicate to the public by telecommunication or on the Internet, loan, distribute and sell theses worldwide, for commercial or non-commercial purposes, in microform, paper, electronic and/or any other formats.

The author retains copyright ownership and moral rights in this thesis. Neither the thesis nor substantial extracts from it may be printed or otherwise reproduced without the author's permission.

AVIS:

L'auteur a accordé une licence non exclusive permettant à la Bibliothèque et Archives Canada de reproduire, publier, archiver, sauvegarder, conserver, transmettre au public par télécommunication ou par l'Internet, prêter, distribuer et vendre des thèses partout dans le monde, à des fins commerciales ou autres, sur support microforme, papier, électronique et/ou autres formats.

L'auteur conserve la propriété du droit d'auteur et des droits moraux qui protège cette thèse. Ni la thèse ni des extraits substantiels de celle-ci ne doivent être imprimés ou autrement reproduits sans son autorisation.

In compliance with the Canadian Privacy Act some supporting forms may have been removed from this thesis.

While these forms may be included in the document page count, their removal does not represent any loss of content from the thesis.

Conformément à la loi canadienne sur la protection de la vie privée, quelques formulaires secondaires ont été enlevés de cette thèse.

Bien que ces formulaires aient inclus dans la pagination, il n'y aura aucun contenu manquant.

Canada

ABSTRACT

Fault Tolerant Control for Bimodal Piecewise Affine Systems

Nastaran Nayebpanah

This thesis addresses the design of fault-tolerant controllers and a fault identification technique for bimodal piecewise affine systems. A new fault-tolerant control methodology is presented. Fault-tolerant, state feedback controllers are synthesized for piecewise-affine (PWA) systems while minimizing an upper bound on the expected value of a quadratic cost function. The controllers are designed to deal with partial loss of control authority in the closed loop PWA system. The proposed controller design technique stabilizes and satisfies performance bounds for both the nominal and faulty systems. Another contribution is the development of a fault identification technique for bimodal piecewise affine (PWA) systems. A Luenberger-based observer structure is applied to estimate partial loss of control authority in PWA systems. More specifically, the unknown value of the fault parameter is estimated by an observer equation obtained from a Lyapunov function. The design procedure is formulated as a set of linear matrix inequalities (LMIs) and guarantees asymptotic stability of the estimation error, provided the norm of the input is upper and lower bounded by positive constants. The new PWA identification method is illustrated in a numerical example. As a third contribution, an active fault-tolerant controller structure is proposed for bimodal PWA systems. The new active fault-tolerant controller structure is illustrated in a numerical example.

ACKNOWLEDGEMENTS

I would like to acknowledge my supervisors, Dr. Luis Rodrigues and Dr. Youmin Zhang. This thesis could not have been accomplished without their guidance and support. I am also very grateful to my supervisors for giving me the opportunity to come to Concordia and join their research group. This opportunity helped me very much to start a new life in the beautiful city of Montréal, to get introduced to the rich culture of French-Canadians in Québec and to start learning the beautiful French language.

I am very grateful to Dr. Khashayar Khorasani and Dr. Chun Yi Su as members of my examining committee for their valuable comments that led to many improvements in this thesis. I would also like to thank my husband, Alireza Mehrabian for his unconditional love and support. I was fortunate to have some fantastic friends and colleagues including Niloofar Moradi, Giancarlo Lugio, Scott Casselman, Ralph Koyess, Behnam Gholitabar Omrani and Kyunjae Baik who helped me take breaks from this thesis when I needed. Last but not least, I would like to thank my parents and my brother for their affection and support.

TABLE OF CONTENTS

LIST OF FIGURES

Chapter 1

Introduction

1.1 Motivation

Increasing reliability of complex systems has received much attention for the past two decades. In particular, design of more reliable aircraft is of great importance in order to avoid fatal aircraft accidents. NASA's aviation safety program (AvSP) [41] is an example of the projects that were initiated to fulfill this demand. "AvSP is working to develop advanced, affordable technologies to help make travel safer on commercial airliners and smaller aircraft", as claimed in [41]. Research is conducted on both "accident prevention" and "accident mitigation". In the area of "accident mitigation" the goal is to make accidents more survivable.

Occurrence of faults in any subsystem of an aircraft might result in aircraft accidents and eventually loss of life and property. Thus, measures must be taken to detect and identify these faults and reconfigure the systems or the aircraft to maintain the required performance or reduce the effect of the fault in the system. On the other hand, in order to analyze the pre-fault and post-fault system for recovery, one needs a precise modeling of the system. Most of the complex systems like aircraft exhibit nonlinear behavior.

However, most of the present methods for fault identification and reconfiguration are designed for linear models of the nonlinear systems. Linear models of nonlinear systems are valid only within a small range around the equilibrium point about which the system is linearized. Piecewise affine (PWA) systems are a class of hybrid systems and provide a framework to describe hybrid dynamical systems exhibiting switching. Such switching might be due to the nature of the system such as dead-zone, saturation and hysteresis. Furthermore, PWA modeling is a good approximation technique for nonlinear systems. PWA approximations of nonlinear systems can be used to globally model a nonlinear system to provide the designer with a more precise model of the system and thus a better chance to successfully reconfigure the faulty system. A PWA approximation of nonlinear dynamics works at a global scale yet, locally, it does not have the same complexity of nonlinear dynamics.

This thesis addresses the design of a fault identification mechanism, a fault-tolerant controller and an active fault-tolerant controller structure for bimodal PWA systems.

1.2 Literature Review

1.2.1 Partial Loss of Control Authority

Partial loss of control authority or Loss-of-Effectiveness (LOE) faults occur due to a reduced gain in the mechanisms that drive the control actuators. Particularly, in aircraft, LOE faults might result in less controllable surface movement for a given command signal than in the pre-fault case. Furthermore, LOE faults may be due to a reduction in aerodynamic coefficients and thus generation of less aerodynamic forces for a given control surface movement [47]. The following subsections present some examples of Loss-of-Effectiveness in aircraft control. LOE faults have been widely investigated in the

literature [10], [11], [12].

Loss of Elevator Effectiveness due to Aircraft Icing

Aircraft icing is one of the main problems that causes performance degradation for a horizontal tail. Accumulation of ice in the horizontal tail is a potentially hazardous condition especially during approach and landing while it is working near its performance limits. The main problem that icing causes is a major reduction of the maximum lift for any aerodynamic surface like the vertical tail or the wing. However, aircraft icing is of main concern on the horizontal tail due to the down-wash caused by the wing. Tail icing is generally not observable from the cockpit. Reference [39] addresses a technique for detecting icing on the horizontal tail by continuously estimating elevator control surface effectiveness. Fig. 1.1 taken from [47] shows how the slope of the lift curve and the maximum lift of airfoils reduce when it is contaminated with various ice shapes. Fig. 1.2 borrowed from [48] shows accumulation of ice on the leading edge of a wing.

In the past 50 years, ice has played a role in numerous accidents that have killed crews and passengers and destroyed aircraft. Some examples of icing-related aircraft accidents include the following:

- "A commuter flight impacted terrain during landing in December 1989, in Pasco, Washington, U.S., killing both crew members and all four passengers. The aircraft had been in icing conditions for about 10 minutes on approach.

- A commuter flight went out of control in icing conditions and dived into a soybean field en route to Chicago, Illinois, U.S., in October 1994. killing all 68 aboard." [44]

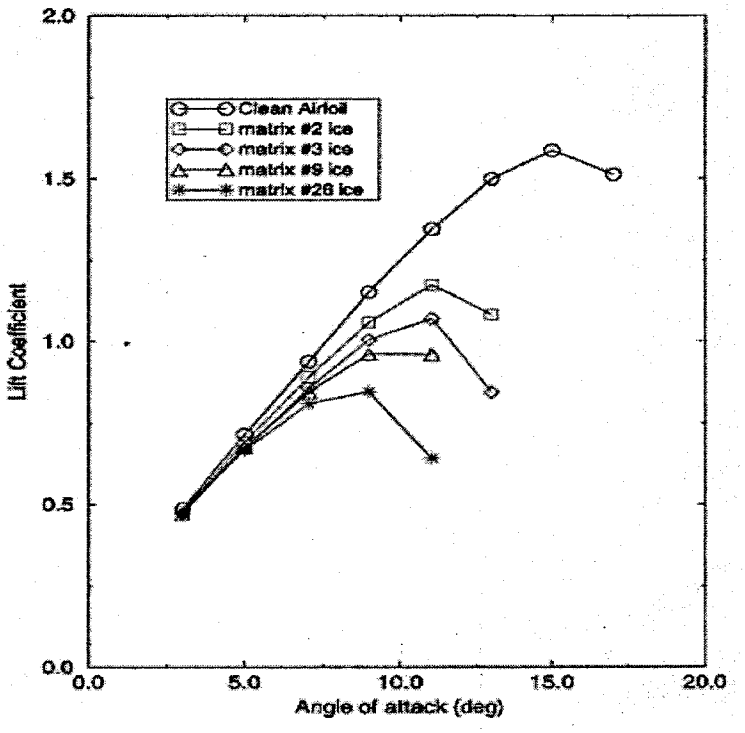

Figure 1.1: Lift curves for clean airfoil and airfoil contaminated with various ice shapes

Loss of Tail-rotor Effectiveness in a Helicopter

Loss of tail-rotor effectiveness (LTE) is a flight characteristic that may result in an uncommanded yaw rate. In order to maintain a constant heading while hovering, the pilot should maintain tail-rotor thrust equal to the trim thrust. The tail-rotor trim thrust, is the thrust required to cancel the effect of the main rotor torque. The required tail-rotor thrust in actual flight is modified by the effects of the wind. If an uncommanded right yaw occurs in flight, it may be because the wind reduced the tail-rotor effective thrust.

The wind can also add to the anti-torque system thrust. In this case, the helicopter will react with an uncommanded left yaw. The wind can and will cause anti-torque system thrust variations to occur [42]. If LTE is not corrected, it results in loss of helicopter control. LTE has been a contributing factor in several helicopter accidents [42]. The

Figure 1.2: Accumulation of ice on wing leading edge

following are examples of accidents due to loss of tail-rotor effectiveness

- "A helicopter collided with the ground following a loss of control during a landing approach. The pilot reported that he was on approach to a ridge line landing zone when, at 70 feet above ground level (AGL) and at an airspeed of 20 knots, a gust of wind induced loss of directional control. The helicopter began to rotate rapidly to the right about the mast. The pilot was unable to regain directional control before ground contact.

- A helicopter entered an uncommanded right turn and collided with the ground. The pilot was maneuvering at approximately 300 feet AGL when the aircraft entered an uncommanded right turn. Unable to regain control, he closed the throttle and attempted an emergency landing into a city park." [42]

1.2.2 Piecewise Affine (PWA) Systems

A system is defined as being "hybrid" when its state has continuous time-driven and discrete event-driven components that evolve with the dynamics of the system. The spread use of computers for the regulation of physical systems with continuous dynamics has spurred the application of hybrid systems in modern engineering [40]. Examples of hybrid systems for aerospace applications are multi-mode aircraft control and gain scheduled control laws. PWA systems are a class of hybrid systems where each i^{th} subsystem is affine:

$$\begin{aligned} \dot{x}(t) &= A_i x(t) + B_i u(t) + m_i \\ y(t) &= C_i x(t) + D_i u(t) \end{aligned} \tag{1.1}$$

where $u(t)$, $x(t)$ and $y(t)$ represent the input, state and output of the system respectively. The matrices A_i, B_i, C_i and D_i and vector of constant values m_i which are called the affine terms, contain real entries. PWA systems provide a framework to describe hybrid dynamical systems exhibiting switching. Such switching might be due to the nature of the system such as dead-zone, saturation and hysteresis. Furthermore, PWA systems may result from piecewise approximations of nonlinear dynamics. Using a PWA model of a complex nonlinear system enables the designer to have a global approximation of the system while locally having simpler affine dynamics. PWA systems pose challenging problems due to their switching nature [28].

State feedback control of continuous-time PWA and piecewise-linear systems have received much attention for the past decade [33], [34], [31]. In [31] analysis and controller synthesis of piecewise linear systems is addressed. In [34] the use of piecewise quadratic cost functions is extended from stability analysis of piecewise linear systems to performance analysis and optimal control. The theory of continuous-time PWA systems has been applied to several different systems, such as, production systems [18], aerospace

systems [19], wheeled robots [21] and electric circuits [22]. In [55] reconfigurable control for PWA systems is addressed. State observer design for general PWA systems was first considered in [58] and later addressed for PWA bimodal systems in [57]. In [23], linear local controllers are extended to PWA controllers that can guarantee global stability. Discrete-time PWA systems have also received attention recently. In [32] a constructive LMI based design procedure for certainty equivalence control of discrete-time PWA systems with continuous dynamics is addressed.

1.2.3 Fault-Tolerant and Reconfigurable Control

In order to increase safety and reliability of safety-critical systems such as aircraft, many researchers have worked on the development of fault-tolerant control systems and reconfigurable control. It is necessary to design control systems which are capable of tolerating potential faults in order to improve the reliability while providing a desirable performance. These types of control systems are often known as fault-tolerant control systems (FTCS) [35]. In [14] an integrated fault detection, diagnosis, and reconfigurable control scheme based on the interacting multiple model (IMM) approach is proposed. Fault detection and diagnosis (FDD) is carried out using an IMM estimator. In [36] an introductory overview on the development of fault-tolerant control systems is presented. [36] summarizes some of the important results in this subject area. Reference [37] provides a perspective on the state of the art in robust approaches to fault-tolerant control and gives some indication of ways in which future research might evolve. In [38] an overview of fault-tolerant control is presented, beginning with robust control, progressing through parallel and analytical redundancy, and ending with rule-based systems and artificial neural networks.

Reconfigurable control acts on-line in response to component faults by restructuring the control loop. Reconfigurable controllers use the estimation of the fault from a

fault detection and identification (FDI) component to correct the faulty system once the fault has been detected and identified [55]. Fault-tolerant and reconfigurable control has been a subject of research since the initial research on restructurable control and self-repairing flight control systems in the early 1980s [45]. An early review on the design issues for fault-tolerant controller synthesis for aircraft was given in 1985 [46]. In [46] the problem of accommodating faults in aircraft is addressed. Techniques which may be used to either passively tolerate or actively detect and compensate for component faults are reviewed, and suggestions are made for integrating these techniques into a restructurable flight control system. A recent review on reconfigurable (active) fault-tolerant control systems (FTCS) is presented in [35]. This thesis proposes a fault-tolerant and a reconfigurable controller design technique. The following definitions for fault-tolerant and reconfigurable control systems in this thesis are now presented.

Definition 1.2.1 *A controller is fault-tolerant when it does not actively detect component faults. Therefore, in the off-line design of fault-tolerant controllers, measures are taken to tolerate potential faults. Note that the design of fault-tolerant controllers is performed off-line and a fault detection and identification (FDI) component is not present in the system. Therefore, a fault-tolerant controller does not have any information about the presence and magnitude of a fault in the system.*

Our next definition is given below.

Definition 1.2.2 *A reconfigurable controller (active fault-tolerant controller) acts on-line in response to component faults. An FDI component provides the information about the presence and the magnitude of a fault in the system. In this thesis, the reconfigurable controller switches among different controller gains based on the information provided by the FDI component.*

1.2.4 Fault Detection and Identification (FDI)

Fault detection addresses the problem of monitoring the occurrence of faults in the system. Fault isolation locates the fault in the system once detected. Fault identification measures the magnitude of the fault in the system. Once the fault is detected, isolated and identified, measures can be taken to mitigate its effect in the system. Many researchers have studied and developed fault detection, isolation and identification (FDI) methods for linear systems. In [53] adaptive observers are applied to detection and isolation of actuator faults in a linear aircraft model. In [13] an approach to detection and diagnosis of multiple faults in a dynamic system is proposed. It is based on the interacting multiple-model (IMM) estimation algorithm. Reference [51] addresses fault detection and isolation for a network of unmanned vehicles using a linear time invariant system representation. In [52] adaptive observers are applied to fault identification and fault-tolerant control of a linear aircraft model. However, dynamical models of most complex systems involve nonlinear phenomena. Some researchers have focused on the development of methodologies to detect and isolate faults for nonlinear systems. In [49] a fault detection and isolation architecture for nonlinear uncertain dynamic systems is presented. This approach uses a bank of nonlinear adaptive estimators. In [50], [54] a methodology for detecting, isolating and accommodating faults in a class of nonlinear dynamic systems is presented. In [55] reconfigurable control of PWA systems after actuator and sensor faults are detected, is addressed. However, [55] does not address fault identification. In [56] an active fault-tolerant control strategy and a fault estimation observer are developed for systems described by multiple linear models. State observer design for general PWA systems was first considered in [58] and later addressed for PWA bimodal systems in [57]. This thesis builds on these previous methods and proposes a fault parameter identification observer for bimodal PWA slab systems. PWA slab systems are a class of PWA systems where switching depends on only

one state of the system. This thesis only addresses identification of the fault parameter. Therefore, a fault detection and isolation logic is not presented.

1.2.5 A Brief Comparison of PWA Systems with Other Switched Systems

A class of switched control systems is Gain Scheduling (GS). In GS, controllers are designed for local linear models of a nonlinear system. In classic GS control, stability of switching among different models is not guaranteed. One extension of the classic GS controller design is so-called Linear Parameter Varying (LPV) modeling and control. This approach enables to obtain linear models of the nonlinear system at different operating points. GS performs a continuous interpolation of the gains while PWA performs discrete switching between a finite number of gains. Another class of switched systems is Takagi-sugeno fuzzy systems. In this class, a convex combination of the controllers for different linear or affine subsystems is used to calculate the controller gains. The convex combination of the controllers is obtained using fuzzy membership functions. Multiple Model (MM) and Interacting Multiple Model (IMM) approaches, include embedded estimators for FDI purposes by using multiple Kalman filters.

1.3 Contributions of the Thesis

The main contributions of this thesis are the following:

- To propose a new fault-tolerant controller synthesis methodology for PWA systems
- To propose a new fault identification mechanism for bimodal PWA systems
- To propose an active fault-tolerant controller structure for bimodal PWA systems

This thesis is mainly based on the following papers:

- N. Nayebpanah, L. Rodrigues, Y. Zhang, "Fault Identification and Reconfigurable Control for Bimodal Piecewise Affine Systems", *European Control Conference – ECC2009*, Budapest, Hungary, 23-26 August, 2009, P: 2694-2699.

- N. Nayebpanah, L. Rodrigues, Y. Zhang, "Fault Detection and Identification for Bimodal Piecewise Affine Systems", *American Control Conference – ACC2009*, St. Louis, Missouri, USA, June 10 - 12, 2009, P: 2362-2366.

- N. Nayebpanah, L. Rodrigues, Y. Zhang, "Fault-Tolerant Controller Synthesis for Piecewise-Affine Systems", *American Control Conference – ACC2009*, St. Louis, Missouri, USA, June 10 - 12, 2009, P: 222-226.

Chapter 2

Fault-Tolerant Controller Synthesis for Piecewise Affine Systems

2.1 Introduction

PWA systems pose challenging problems due to their switching nature [28]. Switching among each closed loop model, either nominal or faulty, may destabilize the system even if each closed loop model is stable and has good performance in its allowed working region [30]. However, if controllers for the PWA nominal and faulty models in all regions are designed together in such a way that there exists a global Lyapunov function for all of them, it is guaranteed that any switching between closed loop PWA models for both nominal and faulty systems will be stable [30]. It is also possible to consider a performance criterion in the controller design problem. In this chapter, an upper bound on the expected value of a quadratic cost function is minimized for all PWA models of both nominal and faulty systems. The controller design criteria is cast as a set of Linear Matrix Inequalities(LMIs) and solved with SeDuMi/YALMIP [59]. The resulting controller will not only handle large deviations from equilibrium points for systems with nonlinear phenomena,

but it also shows a fault-tolerant behavior in the presence of faults without performance degradation for the example in section 2.4.

2.2 Piecewise Affine Representation

Consider a nominal piecewise affine system of the form (2.1). Equation (2.1) might be the natural dynamics of the system or the result of approximating nonlinear dynamics by PWA dynamics.

$$\dot{x}(t) = A_i x(t) + B_i u(t) + m_i \quad \forall x \in \mathscr{R}_i \tag{2.1}$$

In (2.1), $x(t) \in \mathbb{R}^n$ is the state vector of the system, $u(t) \in \mathbb{R}^k$ is the input to the system and $\mathscr{R}_i, i \in \{1,...,M\}$ is a polytopic partition of the state space defined as [28]

$$\mathscr{R}_i = \{x \mid \bar{H}_i \bar{x} > 0\} \tag{2.2}$$

where $\bar{H}_i = \begin{bmatrix} H_i & h_i \\ 0 & 1 \end{bmatrix}$, $\bar{x} = \begin{bmatrix} x \\ 1 \end{bmatrix}$.

For the regions containing the equilibrium points, one has

$$\mathscr{R}_{i0} = \{x \mid H_i x > 0\} \tag{2.3}$$

The vector m_i is the affine term for each affine model which is a constant matrix and $m_i = 0$ for the regions including the equilibrium points.

Ellipsoidal Covering: An exact approximation of the polytopic partitioning of the state space with ellipsoidal cell boundings for the regions that do not contain the equilibrium points can be built for slab systems where switching depends on only one state [28]. This bounding enables a convex formulation of the quadratic stabilization problem for PWA slab systems [28]. The description of the ellipsoidal cells is

$$\mathscr{R}_i \subseteq \varepsilon_i, \quad and \quad \varepsilon_i \subseteq \mathscr{R}_i$$

where

$$\varepsilon_i = \{x \mid \| E_i x + f_i \| < 1\} \tag{2.4}$$

and E_i and f_i follow directly from the polytopic partitioning. More precisely, if $\mathscr{R}_i = \{x \mid d_1 < c_i^T x < d_2\}$, then the associated ellipsoidal cell is described by $E_i = 2c_i^T/(d_2 - d_1)$ and $f_i = -(d_2 + d_1)/(d_2 - d_1)$. A PWA representation for a faulty system with partial loss of control authority is as follows

$$\dot{x}(t) = A_i x(t) + B_{fi} u(t) + m_i \quad \forall x \in \mathscr{R}_i \tag{2.5}$$

The state space partitioning for the faulty system is the same as the nominal system. The matrix B_{fi} encapsulates the fault in the system in each affine model, valid for $\mathscr{R}_i$, $i \in \{1, ..., M\}$. This type of faulty system representation considers partial loss of control authority in all of the actuator channels. Partial loss of control authority is a common type of fault that occurs in certain actuator channels [11, 12, 10]. It can be modeled as a factor that multiplies the B matrix for the nominal system and reduces the amount of control authority. The faulty B matrix modeling partial loss of control authority can be written as

$$B_{fi} = B_i \rho \tag{2.6}$$

where the diagonal matrix ρ is composed of unknown values of partial loss of control authority for $j \in \{1, 2, ..., k\}$ actuators in the system

$$\rho = diag[\rho_1, \rho_2, ..., \rho_k] \tag{2.7}$$

The coefficient ρ_j is a nonzero real number in the unit simplex, i.e, $\rho_j \in (0, 1]$. The case $\rho_j = 0$ corresponding to total loss of control authority is not addressed in this thesis. Therefore, a given value ρ_{jmin} is introduced where ρ_{jmin} is a given value which represents the most severe LOE fault that could happen in the j^{th} actuator channel of the system i.e $\rho_j \in [\rho_{jmin}, 1]$.

2.3 Controller Structure and Performance

It is assumed that for each of the nominal and faulty systems described by equations (2.1) and (2.5), respectively, the state feedback controller is parameterized by $K_i, i \in \{1,...,M\}$ as

$$u = K_i x,\ x \in \mathscr{R}_i. \tag{2.8}$$

A performance criterion will be added to the design considerations to synthesize a guaranteed cost controller [15, 16]

$$J = \int_0^\infty (\bar{x}^T \bar{\Upsilon} \bar{x} + \bar{u}^T \Xi \bar{u}) dt = \int_0^\infty \bar{x}^T (\bar{\Upsilon} + \bar{K_i}^T \Xi \bar{K_i}) \bar{x} dt \quad \forall x \in \mathscr{R}_i \tag{2.9}$$

where $\bar{x} = \begin{bmatrix} x \\ 1 \end{bmatrix}$, $x \in \mathbb{R}^n$ is the state vector of the system, $\bar{u} = \bar{K_i}\bar{x}$, $\bar{K_i} = \begin{bmatrix} K_i & 0 \end{bmatrix}$, $\bar{\Upsilon} = \begin{bmatrix} \Upsilon & 0 \\ 0 & 0 \end{bmatrix}$, and $\Upsilon \geq 0$ and $\Xi > 0$ are weighting matrices.

Theorem 1: An upper bound of the expected value of the cost function (2.9) over random initial conditions verifying

$$\mathbb{E}\{x(0)x^T(0)\} = I, \quad \mathbb{E}\{x(0)\} = 0 \tag{2.10}$$

is minimized for the PWA system (2.1) in closed loop with the controller (2.8) if there is a solution to

$$\begin{aligned} &\min \quad \text{Trace}(P) \\ &s.t. \quad P > 0 \qquad \text{and} \quad (2.11) \quad \forall x \in \mathscr{R}_i \end{aligned}$$

where, $\forall x \in \mathscr{R}_i$, (2.11) is given by

$$\begin{bmatrix} x \\ 1 \end{bmatrix}^T \begin{bmatrix} (A_i+B_iK_i)^TP+P(A_i+B_iK_i) & Pm_i \\ m_i^TP & 0 \end{bmatrix} \begin{bmatrix} x \\ 1 \end{bmatrix} < - \begin{bmatrix} x \\ 1 \end{bmatrix}^T \begin{bmatrix} \Upsilon+K_i^T\Xi K_i & 0 \\ 0 & 0 \end{bmatrix} \begin{bmatrix} x \\ 1 \end{bmatrix} \tag{2.11}$$

Proof: We define a global quadratic candidate Lyapunov function as

$$V(x) = x^TPx \tag{2.12}$$

where $P = P^T > 0$. The derivative of (2.12) for the PWA system (2.1) in closed loop with the controller (2.8) is

$$\dot{V}(t) = [(A_i+B_iK_i)x(t)+m_i]^TPx(t)+x^T(t)P[(A_i+B_iK_i)x(t)+m_i] \quad \forall x \in \mathscr{R}_i \tag{2.13}$$

which can be written in matrix form as follows

$$\dot{V}(t) = \begin{bmatrix} x \\ 1 \end{bmatrix}^T \begin{bmatrix} (A_i+B_iK_i)^TP+P(A_i+B_iK_i) & Pm_i \\ m_i^TP & 0 \end{bmatrix} \begin{bmatrix} x \\ 1 \end{bmatrix} \quad \forall x \in \mathscr{R}_i \tag{2.14}$$

It is required that

$$\bar{x}^T \begin{bmatrix} (A_i+B_iK_i)^TP+P(A_i+B_iK_i) & Pm_i \\ m_i^TP & 0 \end{bmatrix} \bar{x} \leq -\bar{x}^T(\bar{\Upsilon}+\bar{K}_i^T\Xi\bar{K}_i)\bar{x} \quad \forall x \in \mathscr{R}_i \tag{2.15}$$

therefore,

$$\frac{d}{dt}(x^TPx) \leq -\bar{x}^T(\bar{\Upsilon}+\bar{K}_i^T\Xi\bar{K}_i)\bar{x} \quad \forall x \in \mathscr{R}_i \tag{2.16}$$

Multiplying both sides of (2.16) by minus one yields,

$$\bar{x}^T(\bar{\Upsilon}+\bar{K}_i^T\Xi\bar{K}_i)\bar{x} \leq -\frac{d}{dt}(x^TPx) \quad \forall x \in \mathscr{R}_i$$

Integrating both sides yields

$$\int_0^\infty \bar{x}^T(\bar{\Upsilon}+\bar{K}_i^T\Xi\bar{K}_i)\bar{x}dt \leq \int_0^\infty -\frac{d}{dt}(x^TPx) \quad \forall x \in \mathscr{R}_i \tag{2.17}$$

Note that $\lim_{t\to\infty} x(t) \to 0$. In fact, the Lyapunov function (2.12) is positive definite and $V(x) \to \infty$ as $||x|| \to \infty$. The derivative of the Lyapunov function $\dot{V}(x(t))$ is required to be negative definite in inequality (2.15). Therefore, for the system (2.1) the equilibrium at the origin is globally asymptotically stable and therefore $\lim_{t\to\infty} x(t) \to 0$. Using this fact in (2.17) yields

$$J \leq x^T(0)Px(0) \tag{2.18}$$

For random initial conditions note that [15]

$$\mathbb{E}\{J\} \leq \mathbb{E}\{x^T(0)Px(0)\} \tag{2.19}$$

where $\mathbb{E}$ is the expected value operator over random initial conditions $x(0)$ verifying (2.10). We now show that $\mathbb{E}\{x^T(0)Px(0)\}$ is equal to Trace(P). Following the reasoning in [43],

$$\mathbb{E}\{x^T(0)Px(0)\} = \text{Trace}(\mathbb{E}\{x^T(0)Px(0)\}) = \text{Trace}(\mathbb{E}\{x(0)x^T(0)P\})$$

Since,

$$\mathbb{E}\{x(0)x^T(0)\} = I$$

one gets the result

$$\mathbb{E}\{x^T(0)Px(0)\} = \text{Trace}(P)$$

Since $\bar{K}_i = \begin{bmatrix} K_i & 0 \end{bmatrix}$ and $\bar{\Upsilon} = \begin{bmatrix} \Upsilon & 0 \\ 0 & 0 \end{bmatrix}$, the inequality (2.15) can be written as

$\forall x \in \mathscr{R}_i$

$$\begin{bmatrix} x \\ 1 \end{bmatrix}^T \begin{bmatrix} (A_i + B_iK_i)^TP + P(A_i + B_iK_i) & Pm_i \\ m_i^TP & 0 \end{bmatrix} \begin{bmatrix} x \\ 1 \end{bmatrix} < - \begin{bmatrix} x \\ 1 \end{bmatrix}^T \begin{bmatrix} \Upsilon + K_i^T \Xi K_i & 0 \\ 0 & 0 \end{bmatrix} \begin{bmatrix} x \\ 1 \end{bmatrix} \tag{2.20}$$

which is the same as (2.11). This completes the proof. ■

Remark: Inequality condition (2.20) is feasible only in the region $x \in \mathscr{R}_i$. In order to make this condition feasible for all $\forall x \in \mathbb{R}^n$, the S-procedure method [28] is applied in the next theorem.

To formulate controller synthesis as a convex problem one needs the following result.

Theorem 2: For PWA slab systems the inequality (2.11) is implied by the following set of LMIs

$$Q = Q^T > 0, \quad \mu_i < 0, \quad i = 1, ..., M$$

$$\begin{bmatrix} \Gamma_i + \mu_i m_i m_i^T & Q\Upsilon^{1/2} & Y_i^T \Xi^{1/2} & \mu_i m_i f_i^T + Q E_i^T \\ \Upsilon^{1/2} Q & -I_n & 0 & 0 \\ \Xi^{1/2} Y_i & 0 & -I_k & 0 \\ (\mu_i m_i f_i^T + Q E_i^T)^T & 0 & 0 & -\mu_i (1 - f_i f_i^T) \end{bmatrix} < 0 \qquad (2.21)$$

where $\Gamma_i = A_i Q + Q A_i^T + B_i Y_i + Y_i^T B_i^T$.

Proof:

Letting $\mathscr{A}_i = (A_i + B_i K_i)$, (2.11) can be rewritten as

$$\begin{bmatrix} x \\ 1 \end{bmatrix}^T \begin{bmatrix} \mathscr{A}_i^T P + P \mathscr{A}_i & P m_i \\ m_i^T P & 0 \end{bmatrix} \begin{bmatrix} x \\ 1 \end{bmatrix} < - \begin{bmatrix} x \\ 1 \end{bmatrix}^T \begin{bmatrix} \Upsilon + K_i^T \Xi K_i & 0 \\ 0 & 0 \end{bmatrix} \begin{bmatrix} x \\ 1 \end{bmatrix} \quad \forall x \in \mathscr{R}_i \qquad (2.22)$$

Using (2.22) and (2.4) together with the S-procedure with multiplier $\lambda_i < 0$ [28] we observe that (2.22) is implied by

$$\begin{bmatrix} x \\ 1 \end{bmatrix}^T \begin{bmatrix} \mathscr{A}_i^T P + P \mathscr{A}_i + \Upsilon + K_i^T \Xi K_i & P m_i \\ m_i^T P & 0 \end{bmatrix} \begin{bmatrix} x \\ 1 \end{bmatrix} < -\lambda_i \begin{bmatrix} x \\ 1 \end{bmatrix}^T \begin{bmatrix} E_i^T E_i & E_i^T f_i \\ f_i^T E_i & f_i^T f_i - 1 \end{bmatrix} \begin{bmatrix} x \\ 1 \end{bmatrix} \qquad (2.23)$$

Using new variables $Q = P^{-1}$ and $\mu_i = \lambda_i^{-1}$, the sufficient conditions for quadratic stabilization are transformed to

$$Q = Q^T > 0, \;\; \mu_i < 0, \;\; i = 1, ..., M$$

$$\begin{bmatrix} \Pi_i & Q^{-1}m_i + \mu_i^{-1}E_i^T f_i \\ (Q^{-1}m_i + \mu_i^{-1}E_i^T f_i)^T & -\mu_i^{-1}(1 - f_i^T f_i) \end{bmatrix} < 0 \tag{2.24}$$

where

$$\Pi_i = \mathscr{A}_i^T Q^{-1} + Q^{-1}\mathscr{A}_i + \mu_i^{-1}E_i^T E_i + \Upsilon + K_i^T \Xi K_i$$

Applying Schur complement to the inequality (2.24) yields

$$\begin{aligned} &1 - f_i^T f_i < 0 \\ &\Pi_i + (Q^{-1}m_i + \mu_i^{-1}E_i^T f_i)\mu_i(1 - f_i^T f_i)^{-1}(Q^{-1}m_i + \mu_i^{-1}E_i^T f_i)^T < 0 \end{aligned} \tag{2.25}$$

Left multiplying the above inequality by Q, right multiplying it by $Q = Q^T$ and rearranging yields

$$\begin{aligned} &\mathscr{A}_i Q + Q\mathscr{A}_i^T + Q\Upsilon Q + QK_i^T \Xi K_i Q + \mu_i^{-1}QE_i^T E_i Q + \\ &(m_i + \mu_i^{-1}QE_i^T f_i)\mu_i(1 - f_i^T f_i)^{-1}(m_i + \mu_i^{-1}QE_i^T f_i)^T < 0 \end{aligned} \tag{2.26}$$

It was shown in [28] using the Matrix Inversion Lemma that $(1 - f_i^T f_i)^{-1} = 1 + f_i^T (I - f_i^T f_i)^{-1} f_i$. Thus, inequality (2.26) can be rewritten as

$$\begin{aligned} &\mathscr{A}_i Q + Q\mathscr{A}_i^T + Q\Upsilon Q + QK_i^T \Xi K_i Q \\ &+ \mu_i^{-1}QE_i^T E_i Q + \mu_i m_i m_i^T + \mu_i^{-1}(QE_i^T f_i)(QE_i^T f_i)^T \\ &+ m_i(QE_i^T f_i)^T + QE_i^T f_i m_i^T + (\mu_i m_i f_i^T + QE_i^T f_i f_i^T)\mu_i^{-1} \\ &\times (1 - f_i f_i^T)^{-1}(\mu_i m_i f_i^T + QE_i^T f_i f_i^T)^T < 0 \end{aligned} \tag{2.27}$$

Inequality (2.27) can be further rewritten as

$$\begin{aligned}
&\mathscr{A}_i Q + Q\mathscr{A}_i^T + Q\Upsilon Q + QK_i^T \Xi K_i Q + \mu_i m_i m_i^T \\
&+ \mu_i^{-1}(E_i Q)^T (I + f_i f_i^T)(E_i Q) + m_i f_i^T (QE_i^T)^T \\
&+ (QE_i^T)(m_i f_i^T)^T \\
&+ (\mu_i m_i f_i^T + QE_i^T - QE_i^T (I - f_i f_i^T))\mu_i^{-1} \\
&\times (I - f_i f_i^T)^{-1}(\mu_i m_i f_i^T + QE_i^T - QE_i^T (I - f_i f_i^T))^T < 0
\end{aligned} \tag{2.28}$$

Inequality (2.28) can be rearranged as

$$\begin{aligned}
&\mathscr{A}_i Q + Q\mathscr{A}_i^T + Q\Upsilon Q + QK_i^T \Xi K_i Q + \mu_i m_i m_i^T \\
&+ (\mu_i m_i f_i^T + QE_i^T)\mu_i^{-1}(I - f_i f_i^T)^{-1}(\mu_i m_i f_i^T + QE_i^T)^T \\
&+ \mu_i^{-1}(E_i Q)^T (I + f_i f_i^T)(E_i Q) + m_i f_i^T (QE_i^T)^T \\
&+ (QE_i^T)(m_i f_i^T)^T + \mu_i^{-1}(QE_i^T)(I - f_i f_i^T)(QE_i^T)^T \\
&- (\mu_i m_i f_i^T + QE_i^T)\mu_i^{-1} E_i Q - \mu_i^{-1} QE_i^T (\mu_i m_i f_i^T + QE_i^T)^T < 0
\end{aligned} \tag{2.29}$$

which, after simplification, yields

$$\begin{aligned}
&\mathscr{A}_i Q + Q\mathscr{A}_i^T + Q\Upsilon Q + QK_i^T \Xi K_i Q + \mu_i m_i m_i^T \\
&+ (\mu_i m_i f_i^T + QE_i^T)\mu_i^{-1} \\
&\times (I - f_i f_i^T)^{-1}(\mu_i m_i f_i^T + QE_i^T)^T < 0
\end{aligned} \tag{2.30}$$

Using Schur complement and the fact that $1 - f_i^T f_i < 0$ is equivalent to $I - f_i f_i^T < 0$ since f_i is a scalar for PWA slab systems yields

$$\begin{bmatrix} \Lambda_i & \mu_i m_i f_i^T + QE_i^T \\ (\mu_i m_i f_i^T + QE_i^T)^T & -\mu_i(1 - f_i^T f_i) \end{bmatrix} < 0 \tag{2.31}$$

where $\Lambda_i = \mathscr{A}_i Q + Q\mathscr{A}_i^T + \mu_i m_i m_i^T + Q\Upsilon Q + QK_i^T \Xi K_i Q$. Replacing $\mathscr{A}_i$ by $(A_i + B_i K_i)$, introducing a new variable $Y_i = K_i Q$ and using Schur complement yields a convex representation of the sufficient conditions for quadratic stabilization as follows

$$Q = Q^T > 0, \;\; \mu_i < 0, \;\; i = 1, ..., M$$

$$\begin{bmatrix} \Gamma_i + \mu_i m_i m_i^T & Q\Upsilon^{1/2} & Y_i^T \Xi^{1/2} & \mu_i m_i f_i^T + Q E_i^T \\ \Upsilon^{1/2} Q & -I_n & 0 & 0 \\ \Xi^{1/2} Y_i & 0 & -I_k & 0 \\ (\mu_i m_i f_i^T + Q E_i^T)^T & 0 & 0 & -\mu_i (1 - f_i f_i^T) \end{bmatrix} < 0 \qquad (2.32)$$

where $\Gamma_i = A_i Q + Q A_i^T + B_i Y_i + Y_i^T B_i^T$. This completes the proof. ■

In the next corollary, the LMIs in (2.32) are rewritten for a given value of partial loss of control authority ρ_{min} in the system where $\rho_{min} = diag[\rho_{1min}, ..., \rho_{jmin}, ..., \rho_{kmin}]$. ρ_{min} represents the most severe LOE fault matrix in the system. Therefore, the unknown value of the fault parameter in the system (2.5) belongs to the interval of $\rho_j \in [\rho_{jmin}, 1]$.

Corollary 1: For the faulty system with the most severe LOE fault, the inequality (2.32) is transformed to

$$Q = Q^T > 0, \ \mu_i < 0, \ i = 1, ..., M$$

$$\begin{bmatrix} \Gamma_{fi} + \mu_i m_i m_i^T & Q\Upsilon^{1/2} & Y_i^T \Xi^{1/2} & \mu_i m_i f_i^T + Q E_i^T \\ \Upsilon^{1/2} Q & -I_n & 0 & 0 \\ \Xi^{1/2} Y_i & 0 & -I_k & 0 \\ (\mu_i m_i f_i^T + Q E_i^T)^T & 0 & 0 & -\mu_i (1 - f_i f_i^T) \end{bmatrix} < 0 \qquad (2.33)$$

where $\Gamma_{fi} = A_i Q + Q A_i^T + B_{fimin} Y_i + Y_i^T B_{fimin}^T$ and $B_{fimin} = B_i \rho_{min}$.

Proof: It follows trivially by replacing the minimum faulty B_{fimin} matrix into the inequality (2.32). ■

Remark: For the regions $\mathscr{R}_{i0}$ that contain the equilibrium points of the system where $m_i = 0$, the inequalities (2.21) and (2.33) are not strictly feasible and are replaced by

$$\begin{bmatrix} \Gamma_i & Q\Upsilon^{1/2} & Y_i^T\Xi^{1/2} \\ \Upsilon^{1/2}Q & -I_n & 0 \\ \Xi^{1/2}Y_i & 0 & -I_k \end{bmatrix} < 0 \tag{2.34}$$

where $\Gamma_i = A_iQ + QA_i^T + B_iY_i + Y_i^TB_i^T$ and

$$\begin{bmatrix} \Gamma_{fi} & Q\Upsilon^{1/2} & Y_i^T\Xi^{1/2} \\ \Upsilon^{1/2}Q & -I_n & 0 \\ \Xi^{1/2}Y_i & 0 & -I_k \end{bmatrix} < 0 \tag{2.35}$$

where $\Gamma_{fi} = A_iQ + QA_i^T + B_{fimin}Y_i + Y_i^TB_{fimin}^T$ and $B_{fimin} = B_i\rho_{min}$.

Since the P matrix does not directly appear in the inequalities (2.21), (2.33), (2.34) and (2.35), in order to minimize the Trace(P) subject to the mentioned LMIs, it is necessary to add another inequality to show that when the Trace(P) is minimized, the Trace(Q^{-1}) is also minimized. This requires that,

$$\begin{bmatrix} P & I_n \\ I_n & Q \end{bmatrix} > 0 \tag{2.36}$$

According to the Schur complement, this implies

$$P > Q^{-1}$$

Thus, this shows that if the Trace(P) is minimized, then Trace(Q^{-1}) is also minimized. Therefore, to design the controller gains for the guaranteed cost fault-tolerant controller, the following convex problem will be solved.

Definition 2.3.1 Fault-Tolerant Controller *is the solution to the following optimization*

problem

$$\begin{aligned} \min \quad & \text{Trace}(P) \\ s.t. \quad & (2.21),\ (2.33) \quad \forall x \in \mathscr{R}_i \\ & (2.34),\ (2.35) \quad \forall x \in \mathscr{R}_{i0} \\ & (2.36) \end{aligned}$$

From the solution to this problem one gets the controller gains $K_i = Y_i Q^{-1}, i = 1,...,M.$

Remark: In the Linear Matrix Inequalities (2.21) and (2.34) in the Definition 2.3.1, there is no partial loss of control authority fault in the system and therefore $\rho_j = 1$. In the LMIs (2.33) and (2.35), it is assumed that the most severe partial loss of control authority has occurred in the system and therefore, $\rho_j = \rho_{jmin}$ for a given value of ρ_{jmin}. In fact, since these matrix inequalities are convex, therefore, a solution to the optimization problem in 2.3.1 will stabilize the faulty system (2.5) with any LOE fault value belonging to the interval of $\rho_j \in [\rho_{jmin}, 1]$.

2.4 Application to a Wheeled Mobile Robot (WMR)

In this section, the controller design technique that is introduced in this chapter is applied to a path following problem of a WMR. The WMR is shown in Fig. 2.1 and is assumed to be rigid and to be driven by a torque T to control the heading angle ψ of the WMR. The forward velocity $u_0 = 1m/s$ is assumed to be already made constant by the proper design of a cruise controller. The heading angle of the WMR ψ is measured from the positive x-axis in the inertial frame. The kinematic equations of the WMR are

$$\begin{aligned} \dot{y} &= u_0 \sin\psi \\ \dot{\psi} &= R \end{aligned} \tag{2.37}$$

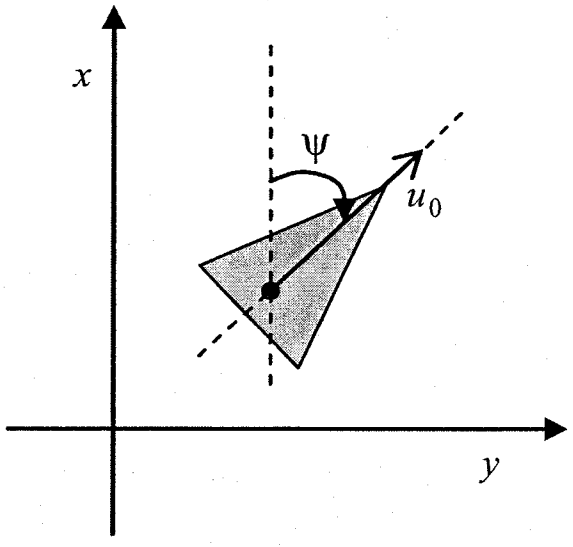

Figure 2.1: Schematic of the Wheeled Mobile Robot (WMR)

The dynamic equation of the WMR is

$$\dot{R} = \frac{1}{I}T \tag{2.38}$$

where T is the input torque generated by the DC motors and is the input to the system. The moment of inertia of the WMR with respect to the center of mass is represented by $I = 1\ kg.m^2$. In this example, it is desired that the WMR follows the path $y = 0$. The above differential equations are cast in matrix form as follows

$$\frac{d}{dt}\begin{bmatrix} y \\ \psi \\ R \end{bmatrix} = \begin{bmatrix} 0 & 0 & 0 \\ 0 & 0 & 1 \\ 0 & 0 & 0 \end{bmatrix}\begin{bmatrix} y \\ \psi \\ R \end{bmatrix} + \begin{bmatrix} u_0 \sin\psi \\ 0 \\ 0 \end{bmatrix} + \begin{bmatrix} 0 \\ 0 \\ 1 \end{bmatrix} T \tag{2.39}$$

Automated methodologies to choose the state space partitioning of piecewise affine systems is addressed in [20]. In this example, piecewise affine models of the system in equation (2.39) are derived for the following state-space partitioning

$$
\begin{aligned}
\mathscr{R}_1 &= \{X \in \mathbb{R}^3 \mid x_2 \in (-\frac{\pi}{15}, \frac{\pi}{15})\} \\
\mathscr{R}_2 &= \{X \in \mathbb{R}^3 \mid x_2 \in (-\frac{\pi}{5}, -\frac{\pi}{15})\} \\
\mathscr{R}_3 &= \{X \in \mathbb{R}^3 \mid x_2 \in (-\frac{3\pi}{5}, -\frac{\pi}{5})\} \\
\mathscr{R}_4 &= \{X \in \mathbb{R}^3 \mid x_2 \in (\frac{\pi}{15}, \frac{\pi}{5})\} \\
\mathscr{R}_5 &= \{X \in \mathbb{R}^3 \mid x_2 \in (\frac{\pi}{5}, \frac{3\pi}{5})\}
\end{aligned}
\tag{2.40}
$$

The criterion to choose the regions in (2.40) is to minimize the approximation error of the system (2.39) by piecewise affine models. The states of the system are $X = \begin{bmatrix} y & \psi & R \end{bmatrix}^T = \begin{bmatrix} x_1 & x_2 & x_3 \end{bmatrix}^T$ with $x_2 = \psi$. The ellipsoidal coverings of the state-space partitioning for the affine regions are

$$
\begin{aligned}
\varepsilon_2 &= \{X \mid \| \begin{bmatrix} 0 & \frac{15}{\pi} & 0 \end{bmatrix} X + 2 \| < 1\} \\
\varepsilon_3 &= \{X \mid \| \begin{bmatrix} 0 & \frac{5}{\pi} & 0 \end{bmatrix} X + 2 \| < 1\} \\
\varepsilon_4 &= \{X \mid \| \begin{bmatrix} 0 & \frac{15}{\pi} & 0 \end{bmatrix} X + 2 \| < 1\} \\
\varepsilon_5 &= \{X \mid \| \begin{bmatrix} 0 & \frac{5}{\pi} & 0 \end{bmatrix} X + 2 \| < 1\}
\end{aligned}
\tag{2.41}
$$

The PWA model for each region is obtained by approximating the nonlinear term $sin(\psi)$ in the system differential equations with a line. The PWA slab models are

$\forall X \in \mathscr{R}_1$

$$
\begin{bmatrix} \dot{y} \\ \dot{\psi} \\ \dot{R} \end{bmatrix} = \begin{bmatrix} 0 & 1 & 0 \\ 0 & 0 & 1 \\ 0 & 0 & 0 \end{bmatrix} \begin{bmatrix} y \\ \psi \\ R \end{bmatrix} + \begin{bmatrix} 0 \\ 0 \\ 0 \end{bmatrix} + \begin{bmatrix} 0 \\ 0 \\ 1 \end{bmatrix} T \tag{2.42}
$$

$\forall X \in \mathscr{R}_2$

$$\begin{bmatrix} \dot{y} \\ \dot{\psi} \\ \dot{R} \end{bmatrix} = \begin{bmatrix} 0 & 0.907 & 0 \\ 0 & 0 & 1 \\ 0 & 0 & 0 \end{bmatrix} \begin{bmatrix} y \\ \psi \\ R \end{bmatrix} + \begin{bmatrix} -0.018 \\ 0 \\ 0 \end{bmatrix} + \begin{bmatrix} 0 \\ 0 \\ 1 \end{bmatrix} T \tag{2.43}$$

$\forall X \in \mathscr{R}_3$

$$\begin{bmatrix} \dot{y} \\ \dot{\psi} \\ \dot{R} \end{bmatrix} = \begin{bmatrix} 0 & 0.2891 & 0 \\ 0 & 0 & 1 \\ 0 & 0 & 0 \end{bmatrix} \begin{bmatrix} y \\ \psi \\ R \end{bmatrix} + \begin{bmatrix} -0.4061 \\ 0 \\ 0 \end{bmatrix} + \begin{bmatrix} 0 \\ 0 \\ 1 \end{bmatrix} T \tag{2.44}$$

$\forall X \in \mathscr{R}_4$

$$\begin{bmatrix} \dot{y} \\ \dot{\psi} \\ \dot{R} \end{bmatrix} = \begin{bmatrix} 0 & 0.907 & 0 \\ 0 & 0 & 1 \\ 0 & 0 & 0 \end{bmatrix} \begin{bmatrix} y \\ \psi \\ R \end{bmatrix} + \begin{bmatrix} 0.018 \\ 0 \\ 0 \end{bmatrix} + \begin{bmatrix} 0 \\ 0 \\ 1 \end{bmatrix} T \tag{2.45}$$

$\forall X \in \mathscr{R}_5$

$$\begin{bmatrix} \dot{y} \\ \dot{\psi} \\ \dot{R} \end{bmatrix} = \begin{bmatrix} 0 & 0.2891 & 0 \\ 0 & 0 & 1 \\ 0 & 0 & 0 \end{bmatrix} \begin{bmatrix} y \\ \psi \\ R \end{bmatrix} + \begin{bmatrix} 0.4061 \\ 0 \\ 0 \end{bmatrix} + \begin{bmatrix} 0 \\ 0 \\ 1 \end{bmatrix} T \tag{2.46}$$

After fault occurrence the PWA model becomes

$\forall X \in \mathscr{R}_1$

$$\begin{bmatrix} \dot{y} \\ \dot{\psi} \\ \dot{R} \end{bmatrix} = \begin{bmatrix} 0 & 1 & 0 \\ 0 & 0 & 1 \\ 0 & 0 & 0 \end{bmatrix} \begin{bmatrix} y \\ \psi \\ R \end{bmatrix} + \begin{bmatrix} 0 \\ 0 \\ 0 \end{bmatrix} + \begin{bmatrix} 0 \\ 0 \\ 1 \end{bmatrix} \rho T \tag{2.47}$$

$\forall X \in \mathscr{R}_2$

$$\begin{bmatrix} \dot{y} \\ \dot{\psi} \\ \dot{R} \end{bmatrix} = \begin{bmatrix} 0 & 0.907 & 0 \\ 0 & 0 & 1 \\ 0 & 0 & 0 \end{bmatrix} \begin{bmatrix} y \\ \psi \\ R \end{bmatrix} + \begin{bmatrix} -0.018 \\ 0 \\ 0 \end{bmatrix} + \begin{bmatrix} 0 \\ 0 \\ 1 \end{bmatrix} \rho T \tag{2.48}$$

$\forall X \in \mathscr{R}_3$

$$\begin{bmatrix} \dot{y} \\ \dot{\psi} \\ \dot{R} \end{bmatrix} = \begin{bmatrix} 0 & 0.2891 & 0 \\ 0 & 0 & 1 \\ 0 & 0 & 0 \end{bmatrix} \begin{bmatrix} y \\ \psi \\ R \end{bmatrix} + \begin{bmatrix} -0.4061 \\ 0 \\ 0 \end{bmatrix} + \begin{bmatrix} 0 \\ 0 \\ 1 \end{bmatrix} \rho T \tag{2.49}$$

$\forall X \in \mathscr{R}_4$

$$\begin{bmatrix} \dot{y} \\ \dot{\psi} \\ \dot{R} \end{bmatrix} = \begin{bmatrix} 0 & 0.907 & 0 \\ 0 & 0 & 1 \\ 0 & 0 & 0 \end{bmatrix} \begin{bmatrix} y \\ \psi \\ R \end{bmatrix} + \begin{bmatrix} 0.018 \\ 0 \\ 0 \end{bmatrix} + \begin{bmatrix} 0 \\ 0 \\ 1 \end{bmatrix} \rho T \tag{2.50}$$

$\forall X \in \mathscr{R}_5$

$$\begin{bmatrix} \dot{y} \\ \dot{\psi} \\ \dot{R} \end{bmatrix} = \begin{bmatrix} 0 & 0.2891 & 0 \\ 0 & 0 & 1 \\ 0 & 0 & 0 \end{bmatrix} \begin{bmatrix} y \\ \psi \\ R \end{bmatrix} + \begin{bmatrix} 0.4061 \\ 0 \\ 0 \end{bmatrix} + \begin{bmatrix} 0 \\ 0 \\ 1 \end{bmatrix} \rho T \tag{2.51}$$

where ρ is an unknown value of partial loss of control authority in the system $\rho \in [0.1, 1]$ and the controller does not receive any information about this unknown value. A fault-tolerant controller is designed for the PWA system (2.47), (2.48), (2.49) using SeDuMi/YALMIP [59]. An LQR controller is also designed for a linear model of the system (2.42) for comparison purposes. The proposed fault-tolerant controller design methodology is compared to the LQR controller, as a controller which is not fault-tolerant. This enables us to observe the fault tolerance capabilities of the proposed fault-tolerant controller design methodology. The LQR controller is designed off-line and does not receive any information about presence or the amount of the fault in the system.

The LQ weighting matrices in the cost function (2.9) are

$$\Upsilon = \begin{bmatrix} 0.1 & 0 & 0 \\ 0 & 0.1 & 0 \\ 0 & 0 & 0.1 \end{bmatrix}$$
$$\Xi = \begin{bmatrix} 0.1 \end{bmatrix} \tag{2.52}$$

The fault-tolerant controller design is based on a maximum of 90% loss of effectiveness in the control authority or $\rho_{min} = 0.1$. The resulting fault-tolerant controllers are

$$\begin{aligned} K_1 &= \begin{bmatrix} -1.0408 & -5.2769 & -9.7329 \end{bmatrix} \\ K_2 = K_4 &= \begin{bmatrix} -1.2946 & -5.0972 & -10.1958 \end{bmatrix} \\ K_3 = K_5 &= \begin{bmatrix} -1.3287 & -5.1018 & -10.2580 \end{bmatrix} \end{aligned} \tag{2.53}$$

with

$$P = \begin{bmatrix} 0.7247 & 1.2181 & 1.3220 \\ 1.2181 & 3.9754 & 5.0744 \\ 1.3220 & 5.0744 & 10.2458 \end{bmatrix} \tag{2.54}$$

The LQR controller is

$$K_{LQR} = \begin{bmatrix} 1.0000 & 2.4142 & 2.4142 \end{bmatrix} \tag{2.55}$$

Simulations are performed for the nonlinear system in feedback with controllers (2.53), with the maximum fault, less severe fault and no fault cases. The resulting paths for the WMR using the fault-tolerant controllers and the LQR controller are plotted in Figs. 2.2, 2.3, 2.10, 2.11. The initial conditions are $\psi_0 = \pi/2, y_0 = 3, R_0 = 0$ for Fig. 2.2 and Fig.2.3 and $\psi_0 = \pi, y_0 = 0, R_0 = 0$ for Fig. 2.10 and Fig. 2.11. Figs. 2.4, 2.5 and 2.6 show the state based switching of the controllers in the simulations with the initial

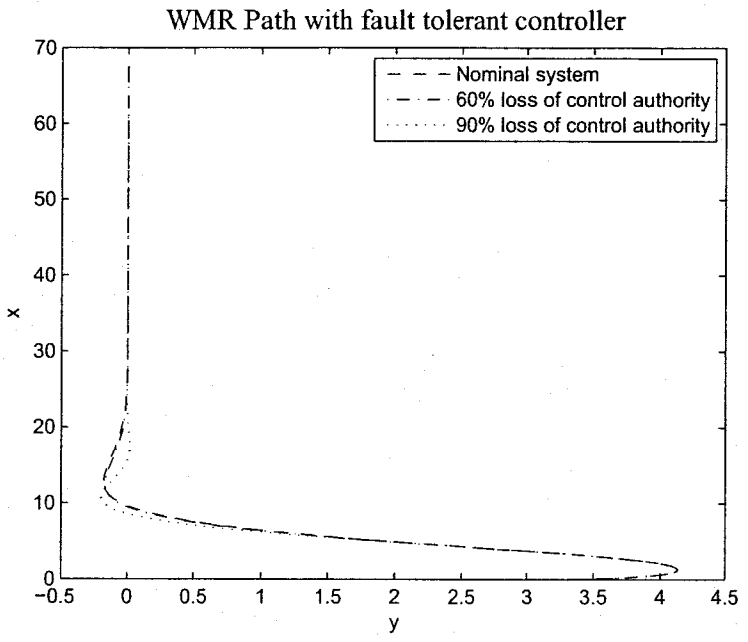

Figure 2.2: WMR following path $y = 0$, FT controller $\psi_0 = \pi/2, y_0 = 3, t_f = 5[sec]$

conditions $\psi_0 = \pi/2$, $y_0 = 3$, $R_0 = 0$. Figs. 2.12, 2.13 and 2.14 show the state based switching of the controllers in the simulations with the initial conditions $\psi_0 = \pi$, $y_0 = 0$, $R_0 = 0$. Fig. 2.7 shows the time variations of the heading angle ψ for the initial conditions $\psi_0 = \pi/2, y_0 = 3, R_0 = 0$ and Fig. 2.15 shows the time variations of the heading angle ψ for the initial conditions $\psi_0 = \pi, y_0 = 0, R_0 = 0$.

Figs. 2.8 and 2.9 show the time response of y with the nominal system and also when a partial loss of control authority of 60% and 90% occurs at $t_f = 5[sec]$. In this case, the initial conditions of the system are $\psi_0 = \pi/2$, $y_0 = 3$, $R_0 = 0$. Figs. 2.16 and 2.17 show the time response of y with the nominal system and also when a partial loss of control authority of 60% and 90% occurs at $t_f = 5[sec]$. In this case, the initial conditions of the system are $\psi_0 = \pi$, $y_0 = 0$, $R_0 = 0$. Figs. 2.20 and 2.21 show the time response of y under the influence of the fault-tolerant and the LQR controllers for an LOE fault of $\rho = 0.2$ occurring at $t_f = 30[sec]$ for square-wave type of desired path.

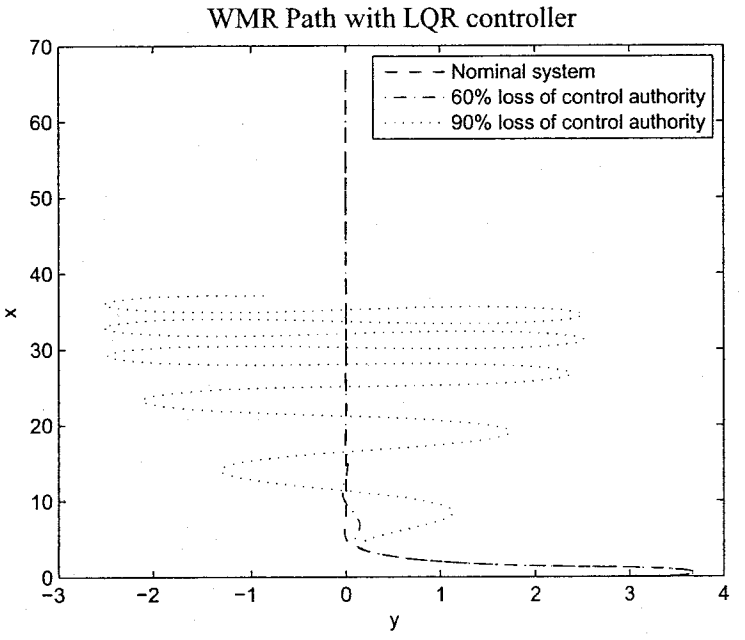

Figure 2.3: WMR following path $y = 0$, LQR controller $\psi_0 = \pi/2, y_0 = 3, t_f = 5[sec]$

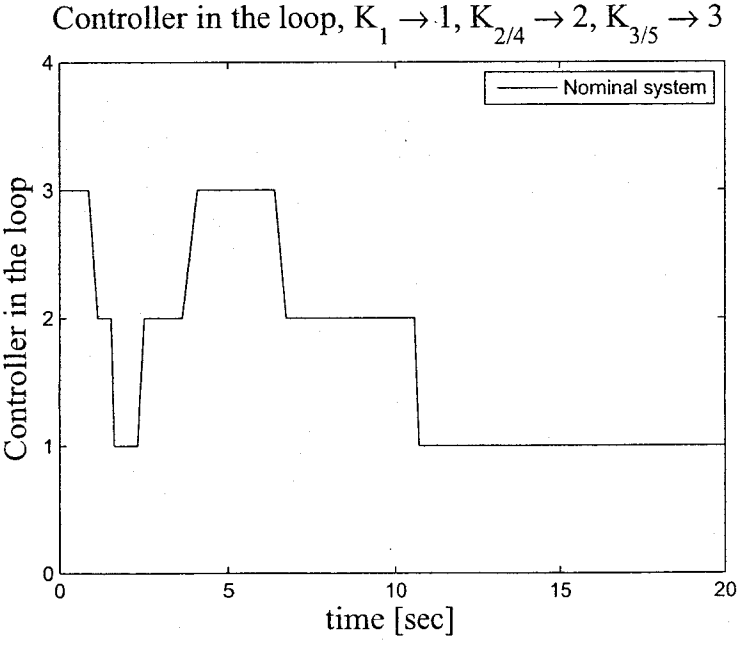

Figure 2.4: Controller in the loop, $\rho = 1$, $\psi_0 = \pi/2, y_0 = 3, t_f = 5[sec]$

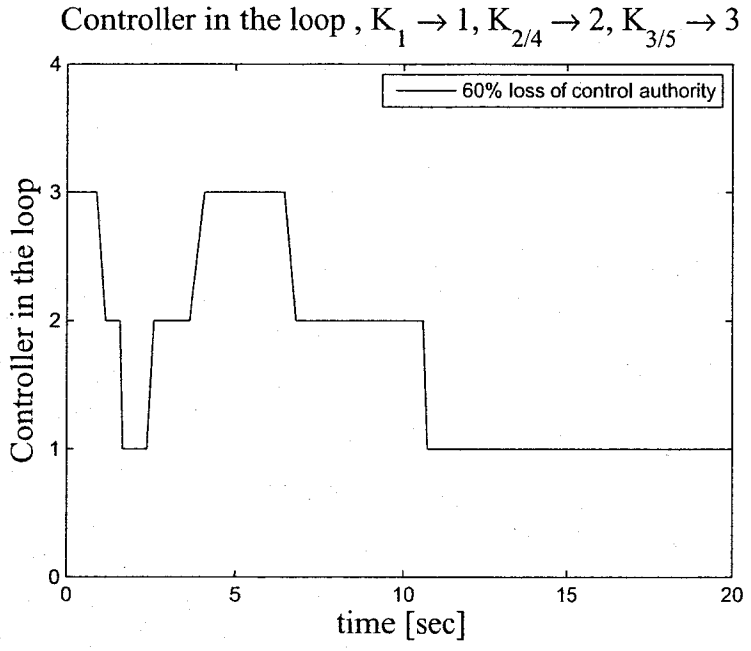

Figure 2.5: Controller in the loop, $\rho = 0.4$, $\psi_0 = \pi/2$, $y_0 = 3$, $t_f = 5[sec]$

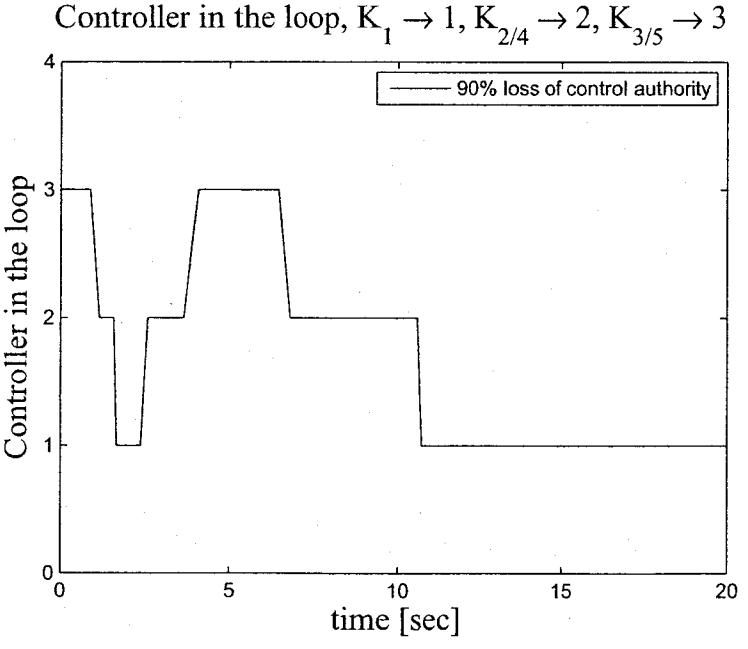

Figure 2.6: Controller in the loop, $\rho = 0.1$, $\psi_0 = \pi/2$, $y_0 = 3$, $t_f = 5[sec]$

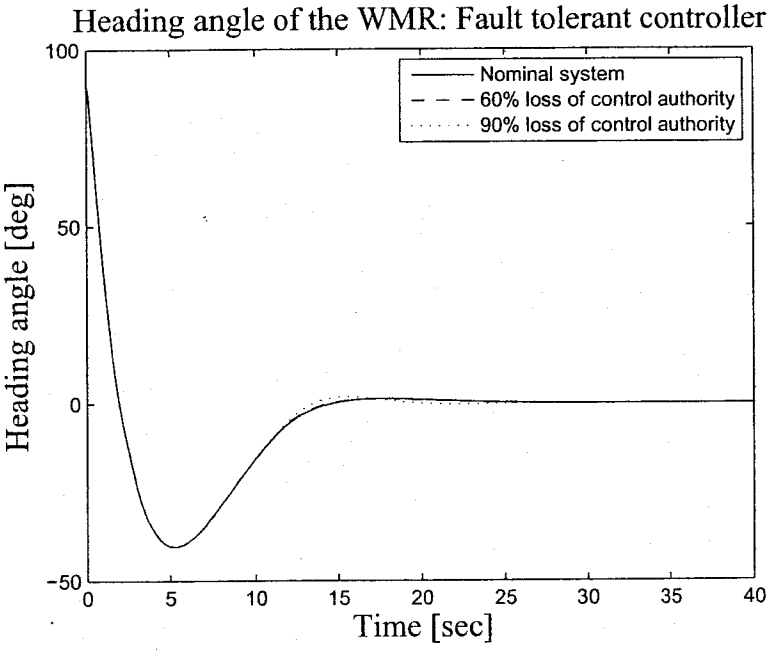

Figure 2.7: Heading angle [deg], $\psi_0 = \pi/2, y_0 = 3, t_f = 5[sec]$

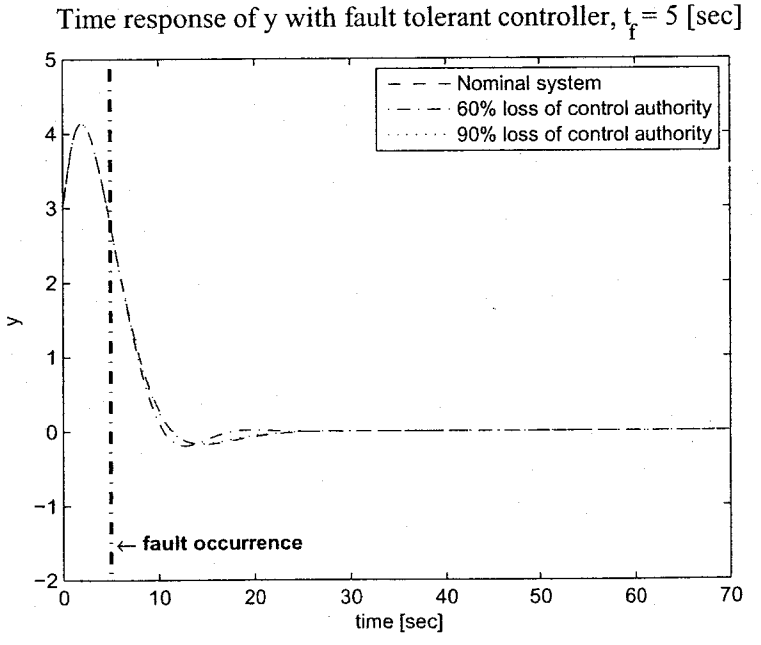

Figure 2.8: Time response of y, $\psi_0 = \pi/2, y_0 = 3, t_f = 5[sec]$

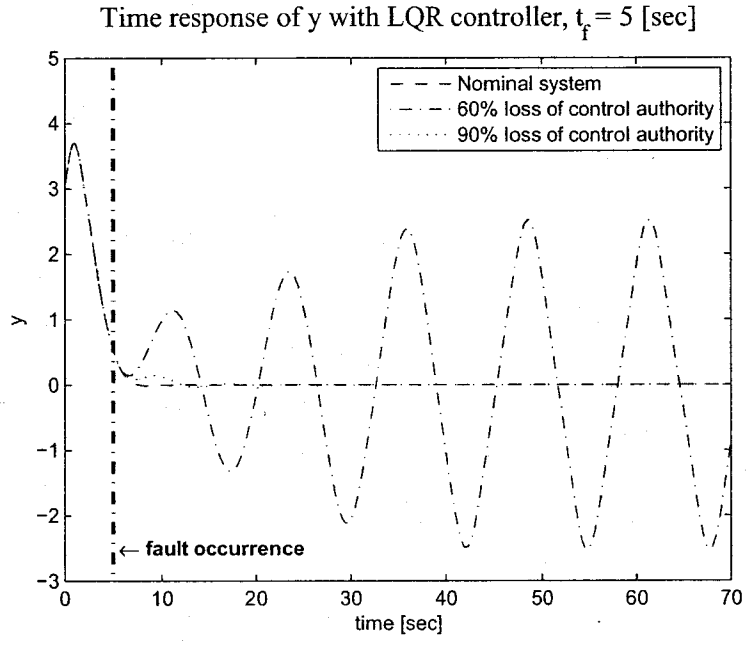

Figure 2.9: Time response of y, $\psi_0 = \pi/2, y_0 = 3, t_f = 5[sec]$

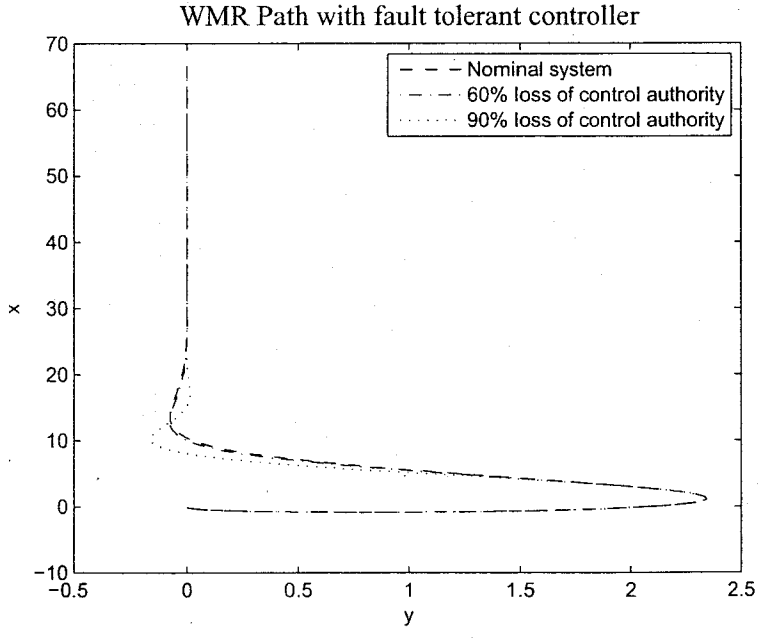

Figure 2.10: WMR following path $y = 0$, FT controller $\psi_0 = \pi, y_0 = 0, t_f = 5[sec]$

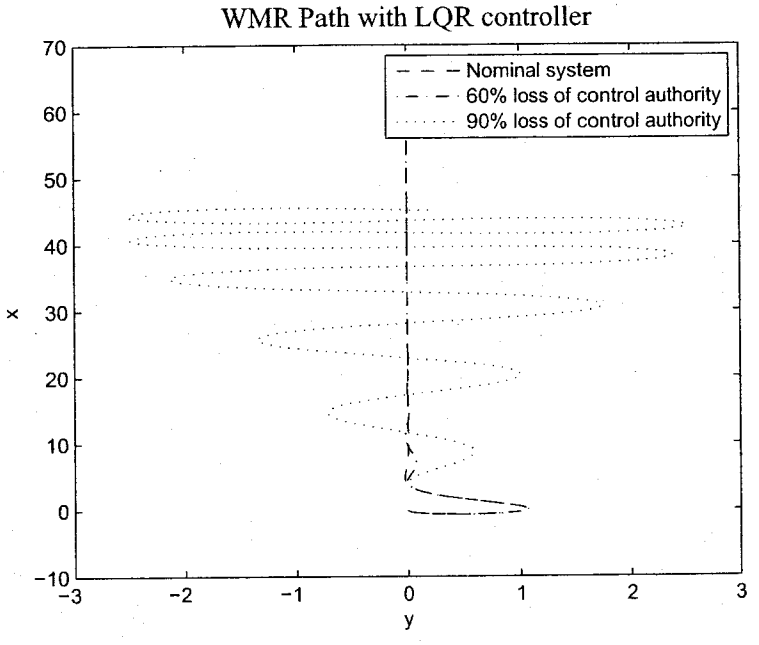

Figure 2.11: WMR following path $y = 0$, LQR controller $\psi_0 = \pi, y_0 = 0, t_f = 5[sec]$

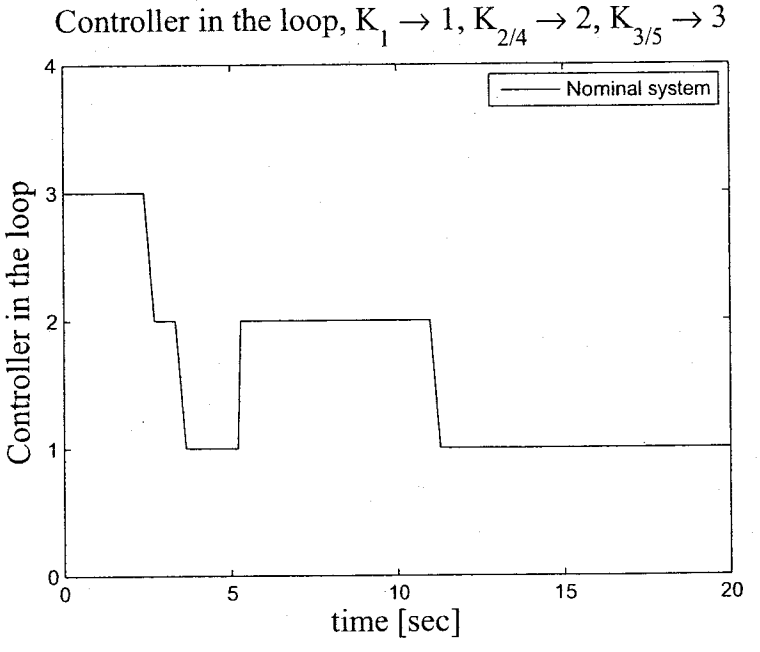

Figure 2.12: Controller in the loop, $\rho = 1$, $\psi_0 = \pi, y_0 = 0, t_f = 5[sec]$

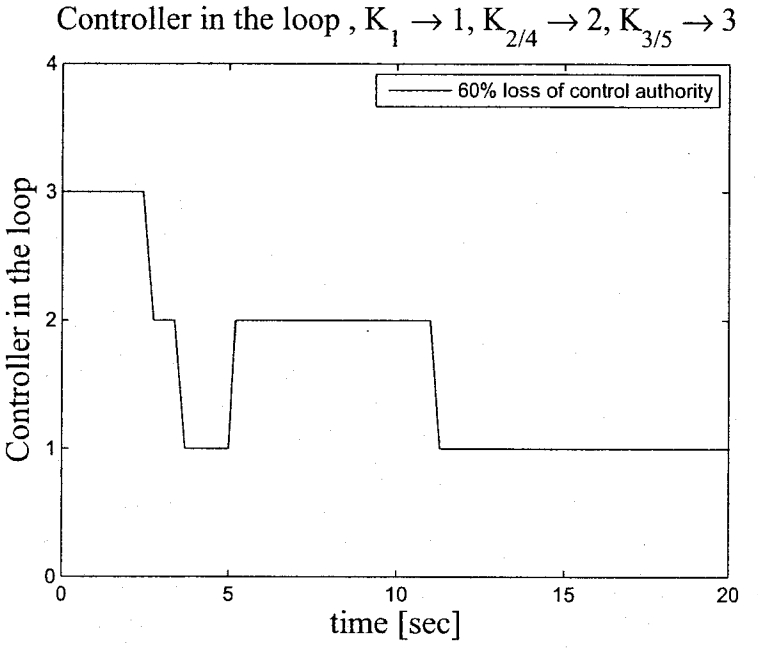

Figure 2.13: Controller in the loop, $\rho = 0.4$, $\psi_0 = \pi, y_0 = 0, t_f = 5[sec]$

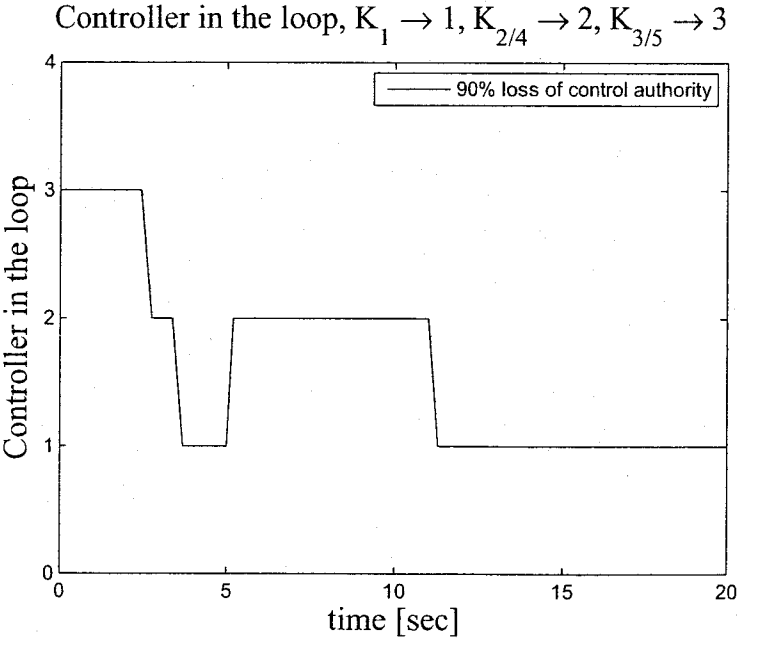

Figure 2.14: Controller in the loop, $\rho = 0.1$, $\psi_0 = \pi, y_0 = 0, t_f = 5[sec]$

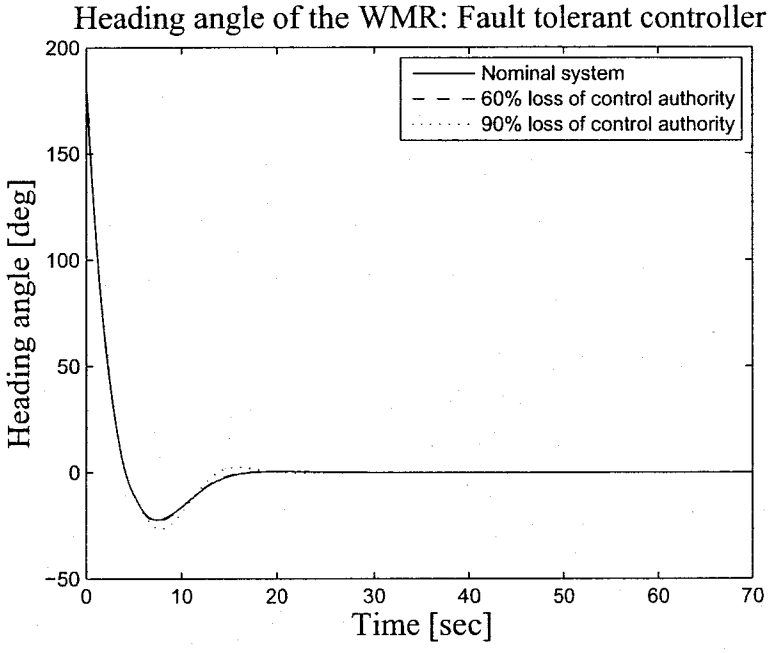

Figure 2.15: Heading angle [deg], $\psi_0 = \pi, y_0 = 0, t_f = 5[sec]$

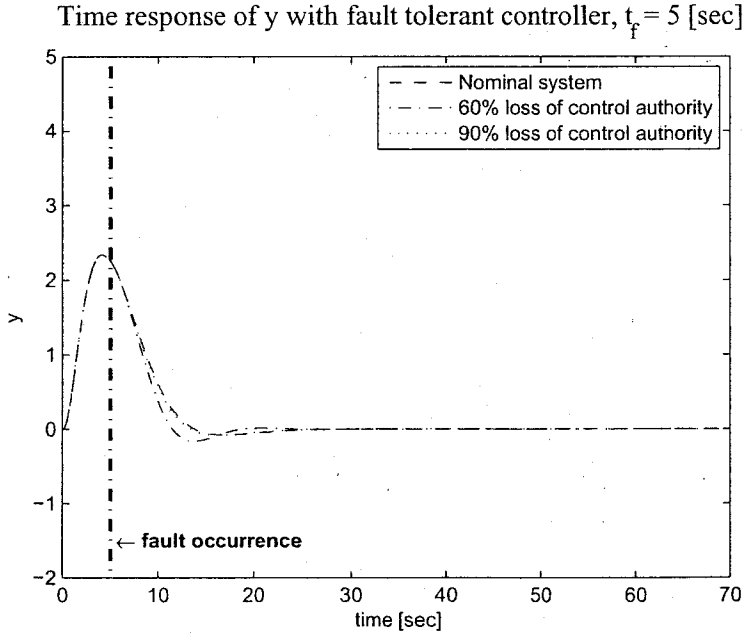

Figure 2.16: Time response of y, $\psi_0 = \pi, y_0 = 0, t_f = 5[sec]$

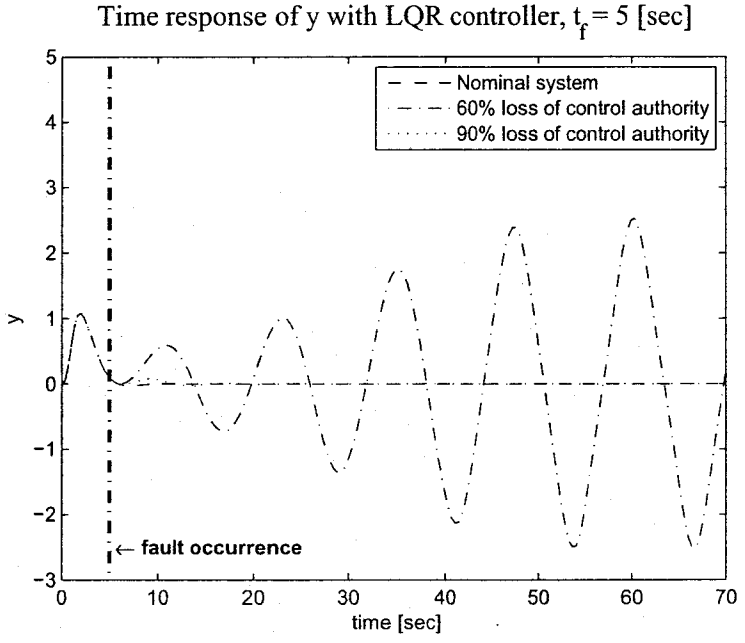

Figure 2.17: Time response of y, $\psi_0 = \pi, y_0 = 0, t_f = 5[sec]$

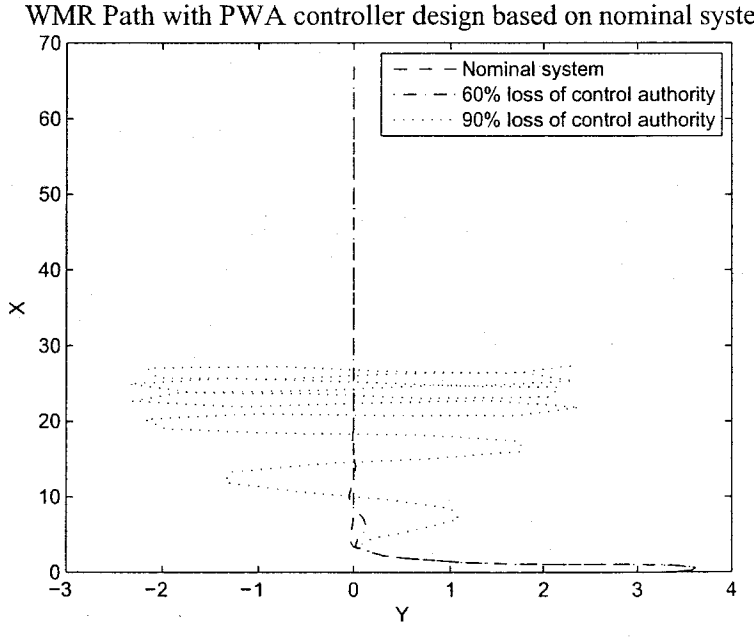

Figure 2.18: WMR following path $y = 0$, controller designed without the LMIs (2.33)

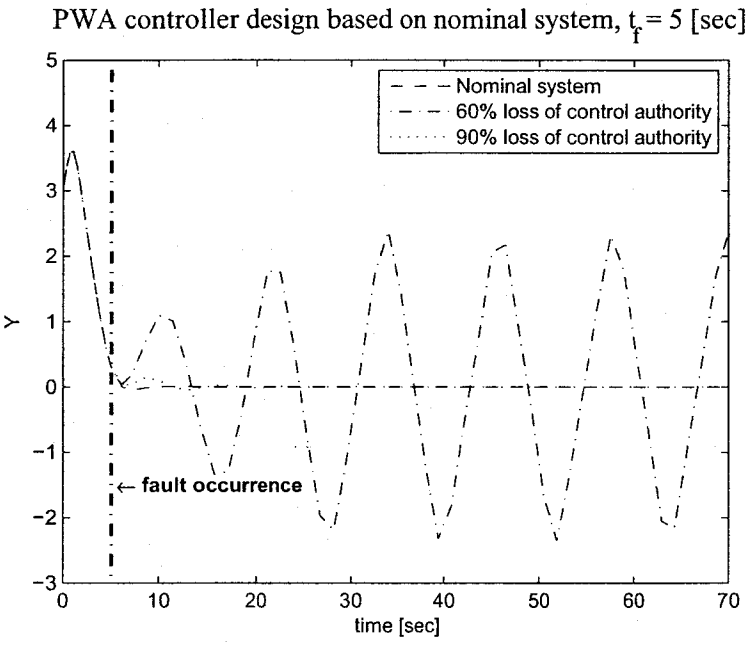

Figure 2.19: Time response of y, controller designed without the LMIs (2.33)

It is observed that the fault-tolerant controllers, which are designed for a PWA model of the system, stabilize the faulty nonlinear system up to 90% partial loss of control authority. It also keeps the performance of the faulty closed loop system the same as the performance of the nominal system. However, as it is observed in the simulations, the LQR controller fails to stabilize the nonlinear system at 90% of loss of control authority.

Furthermore, in order to show the importance of the LMIs (2.33) in fault-tolerance capabilities of the proposed controller design method, for the simulations in the Figs. 2.18 and 2.19 the controllers are designed only with the LMIs in (2.21) with the nominal B matrix. It is observed that the resulting controllers cannot stabilize the system for 90% of loss of control authority, as expected.

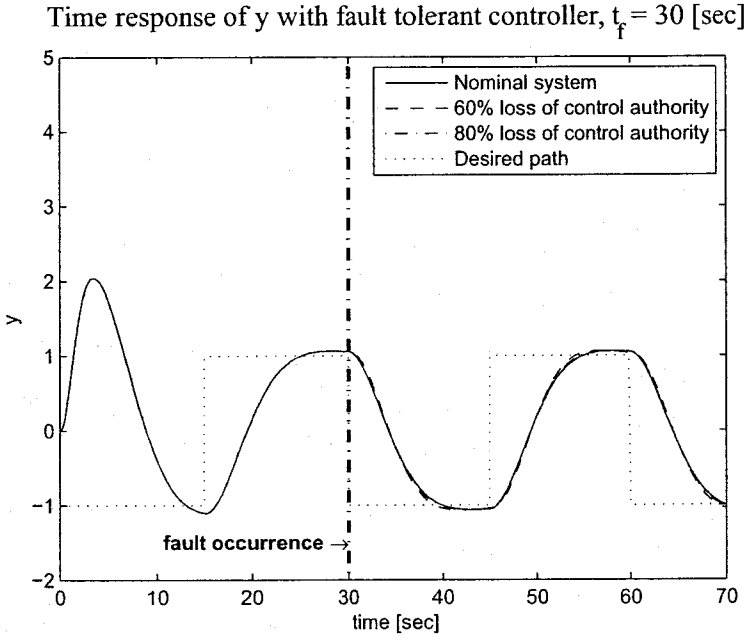

Figure 2.20: Time response of y, $t_f = 30[sec], \rho = 0.2$

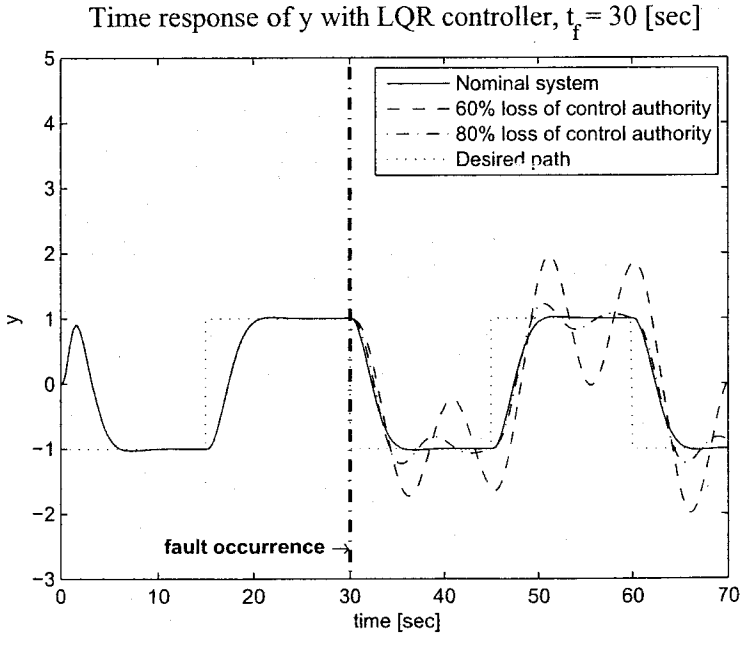

Figure 2.21: Time response of y, $t_f = 30[sec], \rho = 0.2$

2.5 Summary

In this chapter, fault-tolerant controllers are synthesized for PWA systems to deal with LOE faults. A quadratic global Lyapunov function is applied for stability analysis and controller synthesis for PWA nominal and faulty systems. An upper bound on the expected value of the quadratic cost function is minimized for both the nominal and faulty systems. The fault-tolerant controller is capable of stabilizing the PWA system with guaranteed cost performance in the presence of severe LOE faults while an LQR controller is not.

Chapter 3

Fault Identification for Bimodal Piecewise Affine Systems

3.1 Introduction

Increasing reliability of complex systems has received much attention for the past two decades. This interest has spurred a growing demand for fault detection, isolation and identification of complex systems. Fault detection addresses the problem of monitoring the occurrence of a fault in the system. Fault isolation locates the fault in the system once detected. Fault identification measures the magnitude of the fault in the system. Once the fault is detected, isolated and identified, measures can be taken to mitigate its effect in the system. Many researchers have studied and developed fault detection, isolation and identification (FDI) methods for linear systems. In [53] adaptive observers are applied to detection and isolation of actuator faults in a linear aircraft model. Reference [51] addresses fault detection and isolation for a network of unmanned vehicles using a linear time invariant system representation. In [52] adaptive observers are applied to fault identification and fault-tolerant control of a linear aircraft model. However, dynamical

models of most complex systems involve nonlinear phenomena. Therefore, some researchers have focused on the development of methodologies to detect and isolate faults for nonlinear systems. In [49] a fault detection and isolation architecture for nonlinear uncertain dynamic systems is presented. This approach uses a bank of nonlinear adaptive estimators. In [54], [50] a methodology for detecting, isolating and accommodating faults in a class of nonlinear dynamic systems is presented. In [54], the proposed fault diagnosis architecture consists of a fault detection estimator and a bank of isolation estimators, each corresponding to a particular fault type. In [50] a unified methodology for detecting, isolating and accommodating faults in a class of nonlinear dynamic systems is presented.

This chapter addresses identification of the magnitude of a fault in piecewise affine (PWA) slab systems. In PWA slab systems, the switching among several affine or linear models is based on variations of only one state variable in the system. Work on reconfigurable control in PWA systems can be found in [55]. In [55], reconfigurable control of PWA systems after actuator and sensor faults is addressed. However, [55] does not address fault identification. In [56] an active fault-tolerant control strategy and a fault estimation observer are developed for systems described by multiple linear models. However, it does not address PWA systems.

The type of fault considered in this chapter is partial loss of control authority or Loss-of-Effectiveness (LOE). LOE faults occur due to a reduced gain in the mechanisms that drive the control actuators. As examples of LOE faults, the effect of aircraft icing and loss of tail rotor effectiveness in helicopters can be mentioned.

This chapter presents an observer-based fault identification methodology for PWA slab systems. State observer design for general PWA systems was first considered in [58] and later addressed for PWA bimodal systems in [57]. This chapter builds on these previous methods and proposes a fault parameter observer for bimodal PWA slab systems. The observer design is cast as a set of Linear Matrix Inequalities (LMIs) and solved

with SeDuMi/YALMIP [59]. The chapter is organized as follows. First the system and observer structure are introduced. Then, the observer design method is developed. Finally, a numerical example is presented, followed by conclusions.

3.2 System and Observer Structure

Consider a bimodal PWA representation for a PWA system with partial loss of control authority as follows,

$$\begin{cases} \dot{x}(t) = A_1 x(t) + B\rho u(t) & \forall x \in \mathscr{R}_1 \\ y(t) = C_1 x(t) \end{cases}$$

$$\begin{cases} \dot{x}(t) = A_2 x(t) + B\rho u(t) + m_2 & \forall x \in \mathscr{R}_2 \\ y(t) = C_2 x(t) \end{cases} \tag{3.1}$$

where $x(t) \in \mathbb{R}^n$ is the state vector, $u(t) \in \mathbb{R}^k$ is the input and the diagonal matrix ρ is composed of unknown values of partial loss of control authority for k actuators in the system as

$$\rho = diag[\rho_1, \rho_2, ..., \rho_k] \tag{3.2}$$

where $\rho_i \in (0, 1]$. It is assumed that $\mathscr{R}_2$ admits an ellipsoidal description of the form

$$\mathscr{R}_2 = \{x \mid \| E_2 x + f_2 \| < 1\} \tag{3.3}$$

This description can always be found when the two regions have hyperplane boundaries. More precisely, if for example $\mathscr{R}_2 = \{x \mid d_1 < c_2^T x < d_2\}$, then the associated ellipsoidal covering is described by $E_2 = 2c_2^T/(d_2 - d_1)$ and $f_2 = -(d_2 + d_1)/(d_2 - d_1)$. The vector m_2 is the affine term in region $\mathscr{R}_2$ which is a constant matrix. Without loss of generality, the dynamics in region $\mathscr{R}_1$, which contains the equilibrium point of the system, are

considered to be linear, therefore, $m_1 = \mathbf{0}$. The switching of the two subsystems in (3.1) occurs at the boundary of the regions $\mathscr{R}_1$ and $\mathscr{R}_2$ of the state space. The actual input might be reduced by a coefficient matrix ρ due to faults in the system. The structure of the proposed observer is as follows,

$$\begin{cases} \dot{\hat{x}}(t) = A_1\hat{x}(t) + B\hat{\rho}(t)u(t) + G_1(\hat{y}(t) - y(t)) & \forall \hat{x} \in \mathscr{R}_1 \\ \hat{y}(t) = C_1\hat{x}(t) \end{cases}$$

$$\begin{cases} \dot{\hat{x}}(t) = A_2\hat{x}(t) + B\hat{\rho}(t)u(t) + m_2 + G_2(\hat{y}(t) - y(t)) & \forall \hat{x} \in \mathscr{R}_2 \\ \hat{y}(t) = C_2\hat{x}(t) \end{cases} \tag{3.4}$$

where $\hat{y}$, $\hat{\rho}$ and $\hat{x}$ are estimated variables. Depending on the initial conditions of the system and the observer they might or might not work in the same mode. Therefore, the dynamics of the estimation error of the observer $e(t) = \hat{x}(t) - x(t)$ can be divided in four different cases,

Case 1:

$\forall x \in \mathscr{R}_1, \ \forall \hat{x} \in \mathscr{R}_1$

$$\dot{e}(t) = (A_1 + G_1C_1)e(t) + \sum_{i=1}^{k} b_i \, \tilde{\rho}_i(t) \, u_i(t) \tag{3.5}$$

Case 2:

$\forall x \in \mathscr{R}_1, \ \forall \hat{x} \in \mathscr{R}_2$

$$\dot{e}(t) = (A_2 + G_2C_2)e(t) + m_2 + [(A_2 - A_1) + G_2(C_2 - C_1)]x(t) + \sum_{i=1}^{k} b_i \, \tilde{\rho}_i(t) \, u_i(t) \tag{3.6}$$

Case 3:

$\forall x \in \mathscr{R}_2, \ \forall \hat{x} \in \mathscr{R}_1$

$$\dot{e}(t) = (A_1 + G_1C_1)e(t) - m_2 + [(A_1 - A_2) + G_1(C_1 - C_2)]x(t) + \sum_{i=1}^{k} b_i\, \tilde{\rho}_i(t)\, u_i(t) \quad (3.7)$$

Case 4: $\forall x \in \mathscr{R}_2,\ \forall \hat{x} \in \mathscr{R}_2$

$$\dot{e}(t) = (A_2 + G_2C_2)e(t) + \sum_{i=1}^{k} b_i\, \tilde{\rho}_i(t)\, u_i(t) \quad (3.8)$$

where $\tilde{\rho}(t) = \hat{\rho}(t) - \rho$ is the fault estimation error and b_i corresponds the i^{th} column of the B matrix.

Remark: The presented observer design methodology can be extended to general piecewise affine systems with multiple modes following the same reasoning in this chapter. However, the number of the error dynamics equations will grow to n^2 for n number of PWA modes.

Observer design for bimodal systems was addressed in [57]. However, this paper did not address the fault identification problem. The next theorem presents a result on the asymptotic stability of the fault identification observer. In order to proceed, the following assumptions are necessary

- *Assumption 1 (Constant Fault):* Once a fault occurs, its amount remains constant. Thus, $\dot{\rho}_i = 0$ and therefore, $\dot{\tilde{\rho}}_i(t) = \dot{\hat{\rho}}_i(t)$, where i represents the i^{th} control channel.

- *Assumption 2 (Persistent Excitation):* The control input $u(t)$ to the system is upper and lower bounded by positive constants ε_u and $\bar{u}$, i.e, $0 < \varepsilon_u \leq |u(t)| \leq \bar{u}$.

Theorem 1: Suppose that Assumptions 1 and 2 hold. The origin of the observer with the states $(e(t), \tilde{\rho}(t))$ verifying (3.5), (3.6), (3.7), (3.8), (3.9), is asymptotically stable if there exists a positive definite matrix $P = P^T > 0$, matrices W_1, W_2, scalars $\lambda_2 < 0, \lambda_3 < 0$ and fixed positive constants ε and $l_i,\ i = 1, \ldots, k$ such that a solution is obtained for the following design problem.

$$\dot{\hat{\rho}}_i(t) = -l_i e^T(t) P b_i u_i(t) \tag{3.9}$$

$$\begin{aligned} \min \quad & \eta \\ s.t. \quad & \eta > 0,\ \varepsilon I < P < \eta \varepsilon I \\ & (3.10),\ (3.11),\ (3.12),\ (3.13) \end{aligned}$$

where (3.10), (3.11), (3.12) and (3.13) are given by

$$A_1^T P + P A_1 + W_1 C_1 + C_1^T W_1^T \leq 0 \tag{3.10}$$

$$\begin{bmatrix} A_2^T P + P A_2 + W_2 C_2 + C_2^T W_2^T + \lambda_2 E_2^T E_2 & -P\Xi_2 + \lambda_2 E_2^T E_2 & P m_2 + \lambda_2 E_2^T f_2 \\ -\Xi_2^T P + \lambda_2 E_2^T E_2 & \lambda_2 E_2^T E_2 & \lambda_2 E_2^T f_2 \\ m_2^T P + \lambda_2 f_2^T E_2 & \lambda_2 f_2^T E_2 & \lambda_2 (f_2^T f_2 - 1) \end{bmatrix} \leq 0 \tag{3.11}$$

$$\begin{bmatrix} A_1^T P + P A_1 + W_1 C_1 + C_1^T W_1^T & P\Xi_1 & -P m_2 \\ \Xi_1^T P & \lambda_3 E_2^T E_2 & \lambda_3 E_2^T f_2 \\ -m_2^T P & \lambda_3 f_2^T E_2 & \lambda_3 (f_2^T f_2 - 1) \end{bmatrix} \leq 0 \tag{3.12}$$

$$A_2^T P + P A_2 + W_2 C_2 + C_2^T W_2^T \leq 0 \tag{3.13}$$

where $\Xi_1 = (\Delta A + G_1 \Delta C)$, $\Xi_2 = (\Delta A + G_2 \Delta C)$, $\Delta A = A_1 - A_2$, $\Delta C = C_1 - C_2$. From a solution to this problem one gets the observer gains $G_1 = P^{-1} W_1$ and $G_2 = P^{-1} W_2$.

Proof:

Consider a candidate Lyapunov function of the form

$$V(e,\tilde{\rho}) = e^T(t)Pe(t) + \sum_{i=1}^{k} \frac{\tilde{\rho}_i^2(t)}{l_i} \tag{3.14}$$

This function is positive definite because $P = P^T > 0$ and $l_i > 0,\ i = 1,\ldots,k$. To prove stability, we will first show that the derivative of V with respect to time is negative semi-definite and then the set of values for which $\dot{V} = 0$ will be examined in detail. Enforcing that

$$\dot{V} \leq 0,$$

yields

$$\dot{e}^T(t)Pe(t) + e^T(t)P\dot{e}(t) + 2\sum_{i=1}^{k} \frac{\dot{\tilde{\rho}}_i(t)\tilde{\rho}_i(t)}{l_i} \leq 0 \tag{3.15}$$

Replacing the estimation error dynamics (3.5), (3.6), (3.7) and (3.8) into (3.15) yields the following four cases,

Case 1:

$\forall x \in \mathscr{R}_1,\ \ \forall \hat{x} \in \mathscr{R}_1$

$$\begin{aligned} \dot{V} =& e^T(t)[(A_1 + G_1C_1)^T P + P(A_1 + G_1C_1)]e(t) \\ &+ 2\sum_{i=1}^{k} e^T(t)Pb_i\tilde{\rho}_i(t)u_i(t) + 2\sum_{i=1}^{k} \frac{\dot{\tilde{\rho}}_i(t)\tilde{\rho}_i(t)}{l_i} \leq 0 \end{aligned} \tag{3.16}$$

The last two terms in equation (3.16) cancel out each other if $\dot{\tilde{\rho}}_i(t)$ has the structure (3.9). This yields

$$\dot{V} = e^T(t)[(A_1 + G_1C_1)^T P + P(A_1 + G_1C_1)]e(t) \leq 0 \tag{3.17}$$

and thus

$$(A_1 + G_1C_1)^T P + P(A_1 + G_1C_1) \leq 0 \tag{3.18}$$

In order to write the above matrix inequality in a convex form $G_1 = P^{-1}W_1$ is defined. Therefore this replacement in (3.18) yields (3.10).

Case 2:

$\forall x \in \mathscr{R}_1, \ \forall \hat{x} \in \mathscr{R}_2$

In this case, the derivative of the candidate Lyapunov function is

$$\begin{aligned}\dot{V} =& e^T(t)[(A_2 + G_2C_2)^T P + P(A_2 + G_2C_2)]e(t) + x^T(t)[-\Delta A - G_2\Delta C]^T Pe(t) \\ &+ e^T(t)P[-\Delta A - G_2\Delta C]x(t) + m_2^T Pe(t) + e^T(t)Pm_2 \\ &+ 2\sum_{i=1}^{k} \frac{\dot{\tilde{\rho}}_i(t)\tilde{\rho}_i(t)}{l_i} + 2\sum_{i=1}^{k} e^T(t)Pb_i\tilde{\rho}_i(t)u_i(t)\end{aligned} \tag{3.19}$$

The suggested structure for $\dot{\tilde{\rho}}_i(t)$ in case 2 is also (3.9). The remaining terms in the candidate Lyapunov function are written in matrix form as

$$\dot{V} = \begin{bmatrix} e(t) \\ x(t) \\ 1 \end{bmatrix}^T \begin{bmatrix} (A_2 + G_2C_2)^T P + P(A_2 + G_2C_2) & -P[\Delta A + G_2\Delta C] & Pm_2 \\ -[\Delta A + G_2\Delta C]^T P & 0 & 0 \\ m_2^T P & 0 & 0 \end{bmatrix} \begin{bmatrix} e(t) \\ x(t) \\ 1 \end{bmatrix} \leq 0 \tag{3.20}$$

From the fact that for case 2, the state of the system x is in $\mathscr{R}_1$ and the state of the observer $\hat{x}$ is in $\mathscr{R}_2$, the following inequality can be written.

$$\|E_2\hat{x} + f_2\| < 1 \tag{3.21}$$

It is possible to rewrite the above inequality as follows

$$(E_2\hat{x} + f_2)^T(E_2\hat{x} + f_2) < 1 \tag{3.22}$$

Since $e(t) = \hat{x}(t) - x(t)$ inequality (3.22) can be rewritten as

$$\begin{aligned} & e^T E_2^T E_2 e + e^T E_2^T E_2 x + x^T E_2^T E_2 e + x^T E_2^T E_2 x + e^T E_2^T f_2 \\ & + x^T E_2^T f_2 + f_2^T E_2 e + f_2^T E_2 x + f_2^T f_2 < 1 \end{aligned} \tag{3.23}$$

Thus for $\forall x \in \mathscr{R}_1, \ \forall \hat{x} \in \mathscr{R}_2$,

$$\begin{bmatrix} e(t) \\ x(t) \\ 1 \end{bmatrix}^T \begin{bmatrix} E_2^T E_2 & E_2^T E_2 & E_2^T f_2 \\ E_2^T E_2 & E_2^T E_2 & E_2^T f_2 \\ f_2^T E_2 & f_2^T E_2 & f_2^T f_2 - 1 \end{bmatrix} \begin{bmatrix} e(t) \\ x(t) \\ 1 \end{bmatrix} < 0 \tag{3.24}$$

is obtained. The S-procedure [60] is now applied in order to relax (3.20) for $\hat{x} \in \mathscr{R}_2$ yielding for some $\lambda_2 < 0$

$$\begin{aligned} & \begin{bmatrix} e(t) \\ x(t) \\ 1 \end{bmatrix}^T \begin{bmatrix} (A_2 + G_2 C_2)^T P + P(A_2 + G_2 C_2) & -P[\Delta A + G_2 \Delta C] & P m_2 \\ -[\Delta A + G_2 \Delta C]^T P & 0 & 0 \\ m_2^T P & 0 & 0 \end{bmatrix} \begin{bmatrix} e(t) \\ x(t) \\ 1 \end{bmatrix} < \\ & -\lambda_2 \begin{bmatrix} e(t) \\ x(t) \\ 1 \end{bmatrix}^T \begin{bmatrix} E_2^T E_2 & E_2^T E_2 & E_2^T f_2 \\ E_2^T E_2 & E_2^T E_2 & E_2^T f_2 \\ f_2^T E_2 & f_2^T E_2 & f_2^T f_2 - 1 \end{bmatrix} \begin{bmatrix} e(t) \\ x(t) \\ 1 \end{bmatrix} \end{aligned} \tag{3.25}$$

The replacement of $G_2 = P^{-1} W_2$ in the above inequality yields (3.11).

Case 3:

$\forall x \in \mathscr{R}_2, \ \forall \hat{x} \in \mathscr{R}_1$

In this case, the derivative of the candidate Lyapunov function is

$$\begin{aligned}\dot{V} =& e^T(t)[(A_1+G_1C_1)^TP+P(A_1+G_1C_1)]e(t)+x^T(t)[\Delta A+G_1\Delta C]^TPe(t)\\ &+e^T(t)P[\Delta A+G_1\Delta C]x(t)-m_2^TPe(t)-e^T(t)Pm_2\\ &+2\sum_{i=1}^{k}\frac{\dot{\tilde{\rho}}_i(t)\tilde{\rho}_i(t)}{l_i}+2\sum_{i=1}^{k}e^T(t)Pb_i\tilde{\rho}_i(t)u_i(t)\end{aligned} \tag{3.26}$$

The suggested structure for $\dot{\tilde{\rho}}_i(t)$ in case 3 is also (3.9). The remaining terms in the candidate Lyapunov function are written in matrix form as

$$\dot{V}=\begin{bmatrix}e(t)\\x(t)\\1\end{bmatrix}^T\begin{bmatrix}(A_1+G_1C_1)^TP+P(A_1+G_1C_1) & P[\Delta A+G_1\Delta C] & -Pm_2\\ [\Delta A+G_1\Delta C]^TP & 0 & 0\\ -m_2^TP & 0 & 0\end{bmatrix}\begin{bmatrix}e(t)\\x(t)\\1\end{bmatrix}\le 0 \tag{3.27}$$

From the fact that for case 3, the state of the system x is in $\mathscr{R}_2$ and the state of the observer $\hat{x}$ is in $\mathscr{R}_1$, the following inequality can be written.

$$\|E_2x+f_2\|<1 \tag{3.28}$$

It is also possible to rewrite the above inequality as follows

$$(E_2x+f_2)^T(E_2x+f_2)<1 \tag{3.29}$$

or, alternatively, as

$$x^TE_2^TE_2x+x^TE_2^Tf_2+f_2^TE_2x+f_2^Tf_2<1 \tag{3.30}$$

Thus for $\forall x\in\mathscr{R}_2,\ \forall\hat{x}\in\mathscr{R}_1$,

$$\begin{bmatrix} e(t) \\ x(t) \\ 1 \end{bmatrix}^T \begin{bmatrix} 0 & 0 & 0 \\ 0 & E_2^T E_2 & E_2^T f_2 \\ 0 & f_2^T E_2 & f_2^T f_2 - 1 \end{bmatrix} \begin{bmatrix} e(t) \\ x(t) \\ 1 \end{bmatrix} < 0 \tag{3.31}$$

is obtained. The S-procedure [28] is now applied yielding for some $\lambda_3 < 0$ yielding

$$\begin{bmatrix} e(t) \\ x(t) \\ 1 \end{bmatrix}^T \begin{bmatrix} (A_1 + G_1C_1)^T P + P(A_1 + G_1C_1) & P[\Delta A + G_1 \Delta C] & -Pm_2 \\ [\Delta A + G_1 \Delta C]^T P & 0 & 0 \\ -m_2^T P & 0 & 0 \end{bmatrix} \begin{bmatrix} e(t) \\ x(t) \\ 1 \end{bmatrix} < \\ -\lambda_3 \begin{bmatrix} e(t) \\ x(t) \\ 1 \end{bmatrix}^T \begin{bmatrix} 0 & 0 & 0 \\ 0 & E_2^T E_2 & E_2^T f_2 \\ 0 & f_2^T E_2 & f_2^T f_2 - 1 \end{bmatrix} \begin{bmatrix} e(t) \\ x(t) \\ 1 \end{bmatrix} \tag{3.32}$$

The replacement of $G_1 = P^{-1} W_1$ in the above inequality yields (3.12).

Case 4:

$\forall x \in \mathscr{R}_2, \ \forall \hat{x} \in \mathscr{R}_2$

In this case, the derivative of the candidate Lyapunov function is:

$$\begin{aligned} \dot{V} =& e^T(t)[(A_2 + G_2C_2)^T P + P(A_2 + G_2C_2)]e(t) \\ &+ 2\sum_{i=1}^{k} e^T(t) P b_i \tilde{\rho}_i(t) u_i(t) + 2\sum_{i=1}^{k} \frac{\dot{\tilde{\rho}}_i(t)\tilde{\rho}_i(t)}{l_i} \leq 0 \end{aligned} \tag{3.33}$$

The last two terms in equation (3.33) cancel out each other if $\dot{\tilde{\rho}}_i(t)$ has the structure (3.9). This yields

$$\dot{V} = e^T(t)[(A_2 + G_2C_2)^T P + P(A_2 + G_2C_2)]e(t) \leq 0 \tag{3.34}$$

and thus

$$(A_2 + G_2C_2)^T P + P(A_2 + G_2C_2) \leq 0 \tag{3.35}$$

In order to write the above matrix inequality in a convex form $G_2 = P^{-1}W_2$ is defined. Therefore the replacement of G_2 in (3.35) yields inequality (3.13).

Inequalities (3.10), (3.11), (3.12) and (3.13) yield $\dot{V} \leq 0$. Let the set S be defined as

$$S = \{(e, \tilde{\rho}) \mid \dot{V} = 0\} \tag{3.36}$$

For $(e, \tilde{\rho}) \notin S$, $\dot{V} < 0$. Therefore, there exists a time $t > 0$, maybe infinity, for which $(e, \tilde{\rho}) \in S$. But from (3.9), (3.16), (3.19), (3.26) and (3.33), $\dot{V} = 0$ if and only if $e = 0$. If $e = 0, x = \hat{x}$ and the system state will fall under either case 1 or case 4. Since $e = 0$ and the control input has bounded norm by Assumption 2, then the equation for $\dot{\tilde{\rho}}$ in (3.9) yields $\dot{\tilde{\rho}} = 0$, which implies $\tilde{\rho}$ will be constant. This constant value must be zero from the error dynamics (3.5) and (3.8) because $0 \leq \varepsilon_u < |u(t)|$, or otherwise, $e \neq 0$, which would be a contradiction. Therefore, there will be a $t > 0$, maybe infinity, for which the trajectories in the space $(e, \tilde{\rho})$ converge to the origin, proving asymptotic stability. ■

Remark: Notice that one needs the assumption that the control input will not be zero while detecting the fault. This assumption is used in the argument of the proof and it physically corresponds to the need of having persistent excitation. However, this assumption can be relaxed if one asks that the control input be nonzero until the fault is considered to be detected in practice instead of demanding it to be nonzero for all time. Once the fault has been detected, the control input does not need to be persistent anymore and can be equal to zero.

3.3 Application to a Wheeled Mobile Robot (WMR)

In this section, a simplified model of a Wheeled Mobile Robot (WMR) introduced in chapter 2 is used as an example. It is desired that the WMR follows the path shown in Fig. 3.1. The desired path is different from the desired path of the same WMR in the example of chapter 2 since in this chapter, it is necessary to have persistent excitation in the system. Persistent excitation in the PWA system is necessary to enable the observer to identify the partial loss of control authority fault.

PWA models of the system for a regulation problem are derived as

$\forall X \in \mathscr{R}_1$

$$\begin{bmatrix} \dot{x}_1 \\ \dot{x}_2 \\ \dot{x}_3 \end{bmatrix} = \begin{bmatrix} 0 & 1 & 0 \\ 0 & 0 & 1 \\ 0 & 0 & 0 \end{bmatrix} \begin{bmatrix} x_1 \\ x_2 \\ x_3 \end{bmatrix} + \begin{bmatrix} 0 \\ 0 \\ 1 \end{bmatrix} \rho u \tag{3.37}$$

$\forall X \in \mathscr{R}_2$

$$\begin{bmatrix} \dot{x}_1 \\ \dot{x}_2 \\ \dot{x}_3 \end{bmatrix} = \begin{bmatrix} 0 & -0.6366 & 0 \\ 0 & 0 & 1 \\ 0 & 0 & 0 \end{bmatrix} \begin{bmatrix} x_1 \\ x_2 \\ x_3 \end{bmatrix} + \begin{bmatrix} 2 \\ 0 \\ 0 \end{bmatrix} + \begin{bmatrix} 0 \\ 0 \\ 1 \end{bmatrix} \rho u \tag{3.38}$$

where $u = T$ is the torque input, $X = \begin{bmatrix} x_1 & x_2 & x_3 \end{bmatrix}^T = \begin{bmatrix} y & \psi & R \end{bmatrix}^T$ and $\rho \in (0,1]$ is the unknown amount of partial loss of control authority which should be identified by the observer. The state-space partitioning is

$$\begin{aligned} \mathscr{R}_1 &= \{X \in \mathbb{R}^3 \mid x_2 \in (-\frac{\pi}{2}, \frac{\pi}{2})\} \\ \mathscr{R}_2 &= \{X \in \mathbb{R}^3 \mid x_2 \in (\frac{\pi}{2}, \frac{3\pi}{2})\} \end{aligned} \tag{3.39}$$

The state space partitioning in (3.39) is different from the partitions of the example in chapter 2 since in this chapter, it is necessary to choose only two regions in order to have a bimodal PWA system. The criterion for choosing these regions is to minimize the approximation error using two regions.

The ellipsoidal cell of the state-space partitioning is only defined for $\mathscr{R}_2$ where the system is affine

$$\varepsilon_2 = \{X \mid \| \begin{bmatrix} 0 & \frac{2}{\pi} & 0 \end{bmatrix} X - 2 \| < 1\} \tag{3.40}$$

In this example a path-following problem is addressed. Therefore, the tracking error is defined as $\delta(t) = X(t) - X_{des}$ where $X_{des} = \begin{bmatrix} y_{des} & 0 & 0 \end{bmatrix}^T$ and the rate of change of the tracking error as $\dot{\delta}(t) = \dot{X}(t) - \dot{X}_{des}$. It is assumed that $\dot{X}_{des} = \mathbf{0}$. Therefore, $\dot{\delta}(t) = \dot{X}(t)$

$\forall \delta \in \mathscr{R}_1$

$$\begin{bmatrix} \dot{\delta}_1 \\ \dot{\delta}_2 \\ \dot{\delta}_3 \end{bmatrix} = \begin{bmatrix} 0 & 1 & 0 \\ 0 & 0 & 1 \\ 0 & 0 & 0 \end{bmatrix} \begin{bmatrix} \delta_1 \\ \delta_2 \\ \delta_3 \end{bmatrix} + \begin{bmatrix} 0 \\ 0 \\ 1 \end{bmatrix} \rho u \tag{3.41}$$

$\forall \delta \in \mathscr{R}_2$

$$\begin{bmatrix} \dot{\delta}_1 \\ \dot{\delta}_2 \\ \dot{\delta}_3 \end{bmatrix} = \begin{bmatrix} 0 & -0.6366 & 0 \\ 0 & 0 & 1 \\ 0 & 0 & 0 \end{bmatrix} \begin{bmatrix} \delta_1 \\ \delta_2 \\ \delta_3 \end{bmatrix} + \begin{bmatrix} 2 \\ 0 \\ 0 \end{bmatrix} + \begin{bmatrix} 0 \\ 0 \\ 1 \end{bmatrix} \rho u \tag{3.42}$$

where $\delta = \begin{bmatrix} \delta_1 & \delta_2 & \delta_3 \end{bmatrix}^T = \begin{bmatrix} y - y_{des} & \psi & R \end{bmatrix}^T$. Note that $x_2(t) = \delta_2(t) = \psi(t)$. Therefore, the state space partitioning and the ellipsoidal cells from (3.39) and (3.40) still hold for the system of the path-following problem in (3.41) and (3.42).

In order that the WMR follows the desired path, an LQR controller is designed for the linear model of the system in (3.41). In the simulations, a partial loss of control authority occurs while the WMR is following the desired path. The observers which are proposed in this chapter are then applied to estimate the value of partial loss of control authority. The weighting matrices for the LQR controller are

$$Q = \begin{bmatrix} 0.001 & 0 & 0 \\ 0 & 0.001 & 0 \\ 0 & 0 & 0.001 \end{bmatrix}, R = 0.1$$

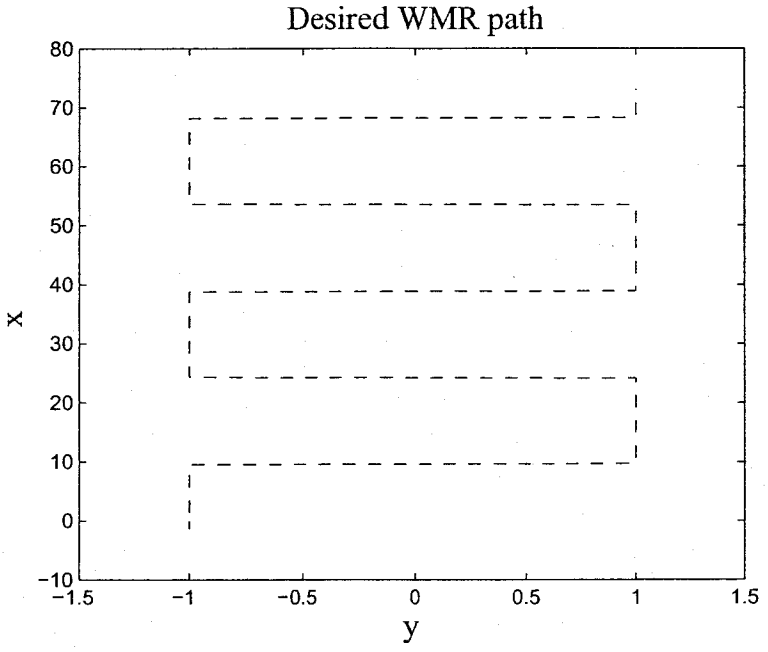

Figure 3.1: WMR desired path

The gains of the LQR controller are

$$K_{LQR} = \begin{bmatrix} 0.1 & 0.447 & 0.951 \end{bmatrix} \tag{3.43}$$

A solution to the observer design problem in Theorem 1 is sought and obtained by SeDuMi/YALMIP [59] as

$$G_1 = \begin{bmatrix} -106929.72722 & 5.53193 & 0.00003 \\ 5.53200 & -21140.12825 & -0.5290 \\ 0.00003 & -0.52900 & -21193.96940 \end{bmatrix} \tag{3.44}$$

$$G_2 = \begin{bmatrix} -106641.67738 & -82.25111 & -0.00028 \\ -82.25096 & -21358.52754 & -0.52855 \\ -0.00028 & -0.52855 & -21472.71741 \end{bmatrix} \tag{3.45}$$

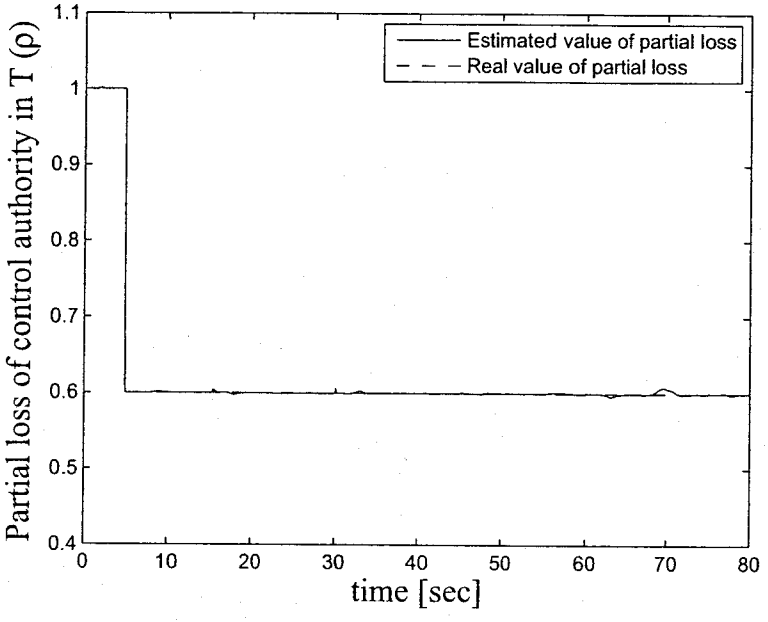

Figure 3.2: Fault identification in torque input T, $t_f = 5[sec]$ and $\rho = 0.6$

$$P = \begin{bmatrix} 3.9999 & 0.0000 & 0.0000 \\ 0.0000 & 3.9999 & 0.0000 \\ 0.0000 & 0.0000 & 3.9999 \end{bmatrix} \tag{3.46}$$

$$\lambda_2 = -8.02107 \times 10^{-5}, \quad \lambda_3 = -7.9994 \times 10^{-5}, \quad \varepsilon = 4 \tag{3.47}$$

Figs. 3.2-3.13 show the simulation results with the structure (3.9). In Fig. 3.2 a fault occurs at $t = 5[sec]$. In Figs. 3.2 and 3.3 the simulated fault is 40% loss of control authority in the input. The input to the system is shown in Fig. 3.3. In Figs. 3.4 and 3.5, 20% loss of control authority occurs at $t = 5[sec]$. In Figs. 3.6 and 3.7, 40% loss of control authority occurs at $t = 15[sec]$. Figs. 3.8 and 3.9 show time variations of the heading angle ψ. Figs. 3.10-3.13 show fault identification and the system inputs for $\rho = 0.9$ (10% loss of control authority) and $\rho = 0.1$ (90% loss of control authority) occurring at $t_f = 30[sec]$.

In these simulations, the input changes sign a few times which means that it has a

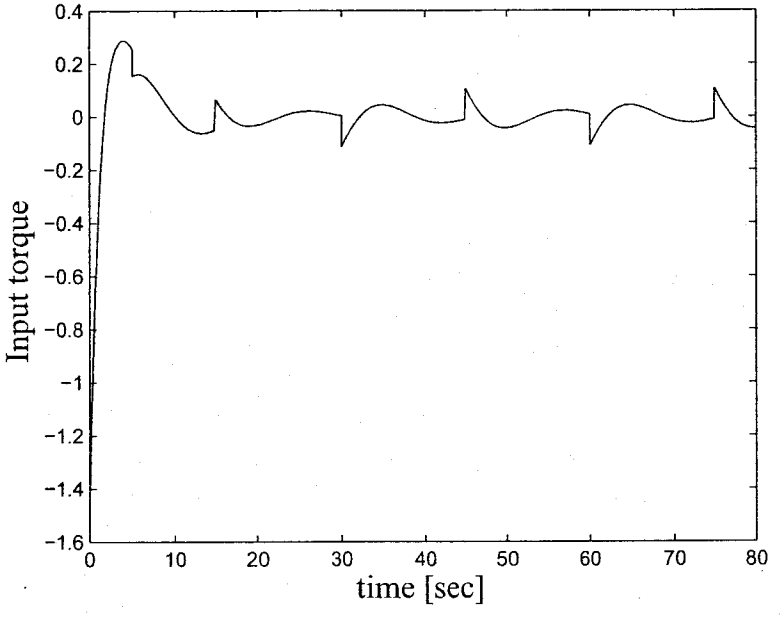

Figure 3.3: System input, $t_f = 5[sec]$ and $\rho = 0.6$

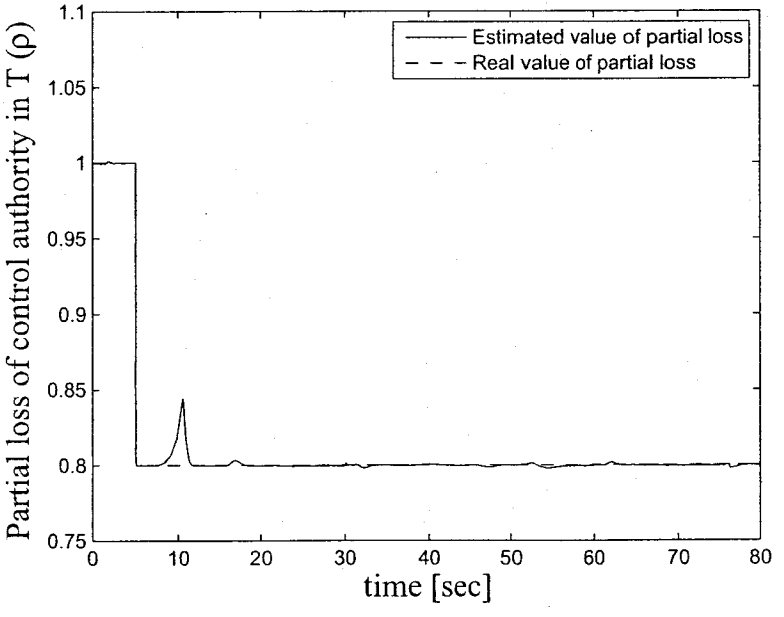

Figure 3.4: Fault identification in torque input T, $t_f = 5[sec]$ and $\rho = 0.8$

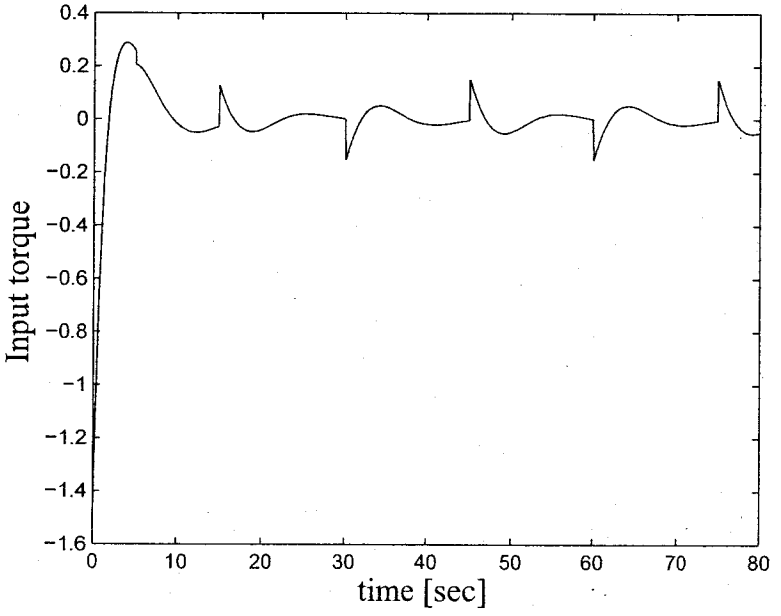

Figure 3.5: System input, $t_f = 5[sec]$ and $\rho = 0.8$

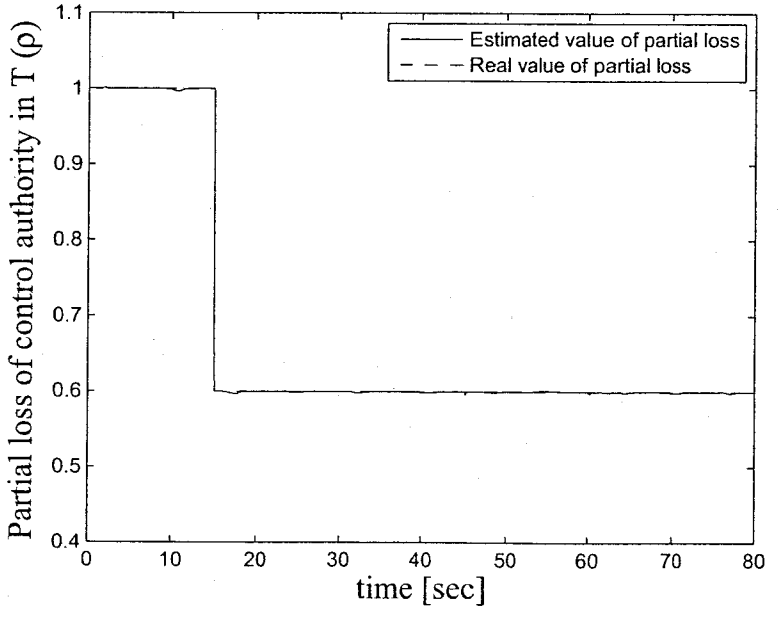

Figure 3.6: Fault identification in torque input T, $t_f = 15[sec]$ and $\rho = 0.6$

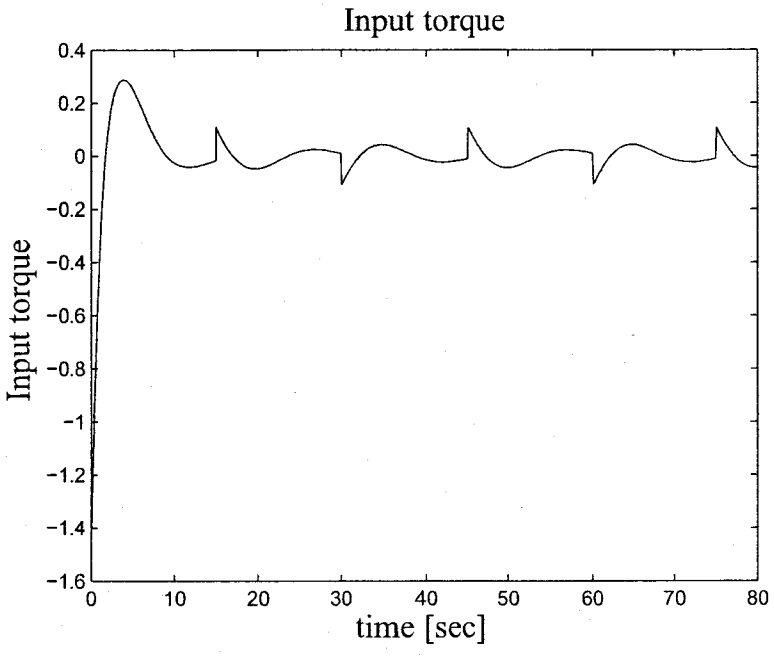

Figure 3.7: System input $t_f = 15[sec]$ and $\rho = 0.6$

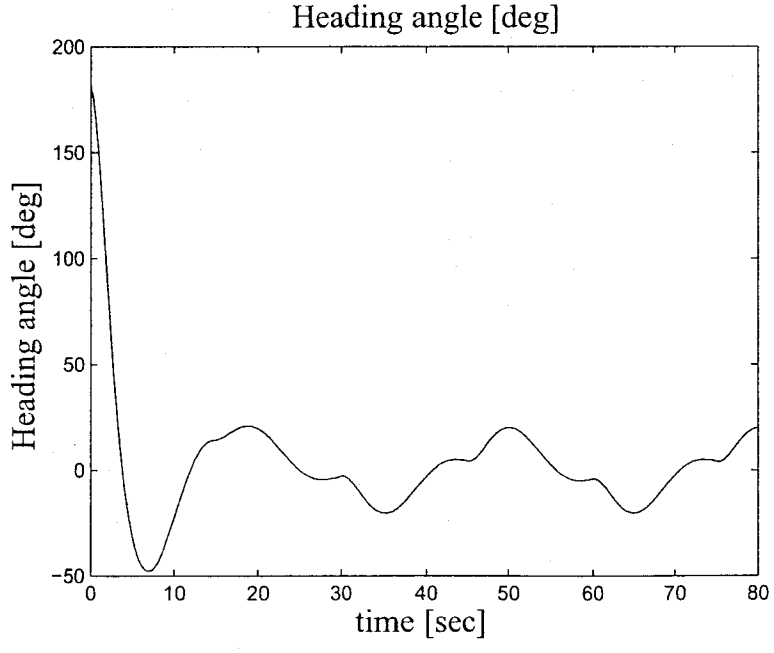

Figure 3.8: $\psi(t)$ [deg] for $t_f = 5[sec]$ and $\rho = 0.6$

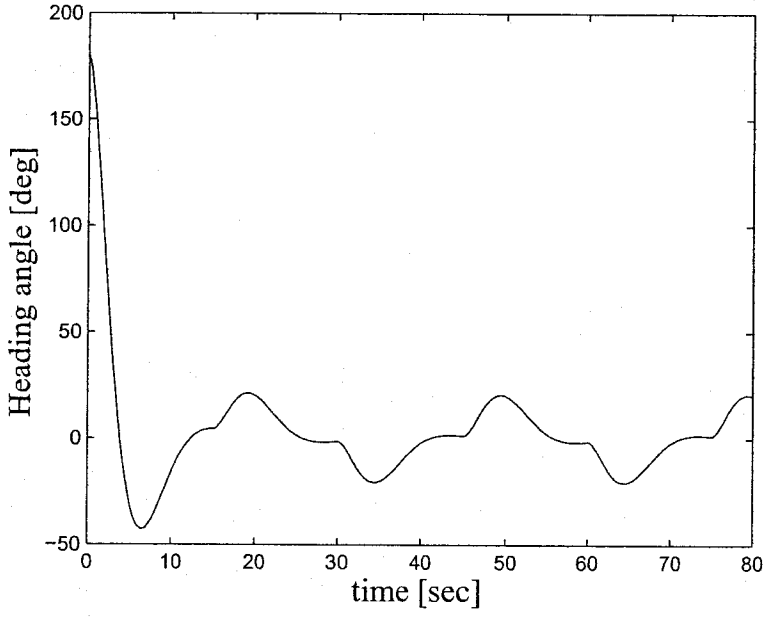

Figure 3.9: $\psi(t)$ [deg] for the nominal system

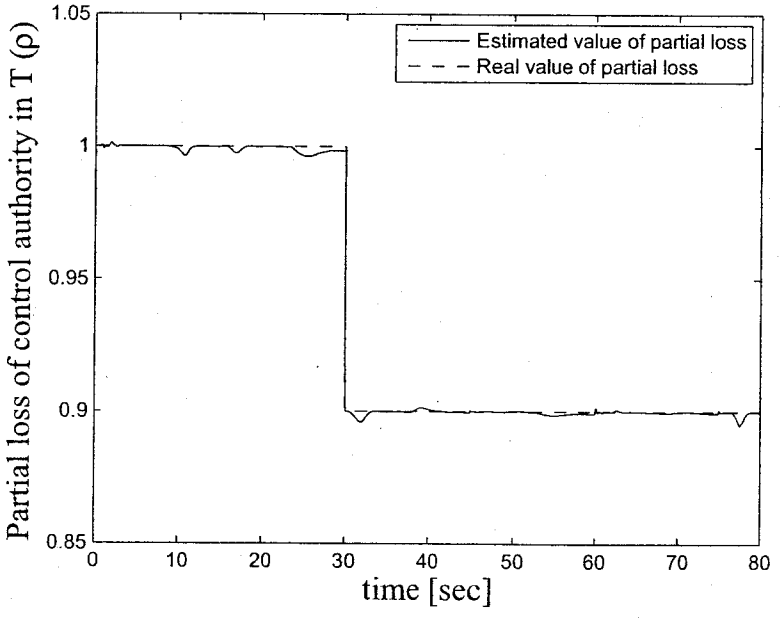

Figure 3.10: Fault identification in torque input T, $t_f = 30[sec]$ and $\rho = 0.9$

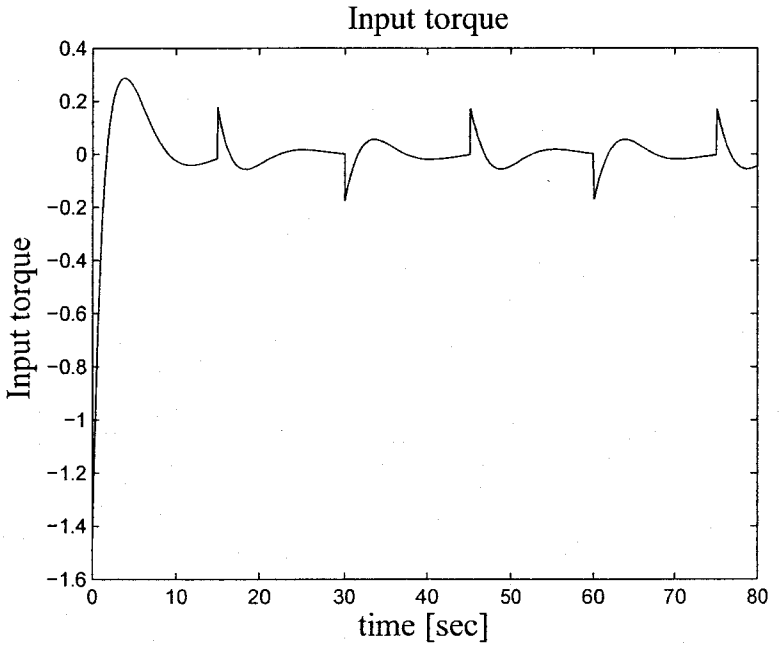

Figure 3.11: System input $t_f = 30[sec]$ and $\rho = 0.9$

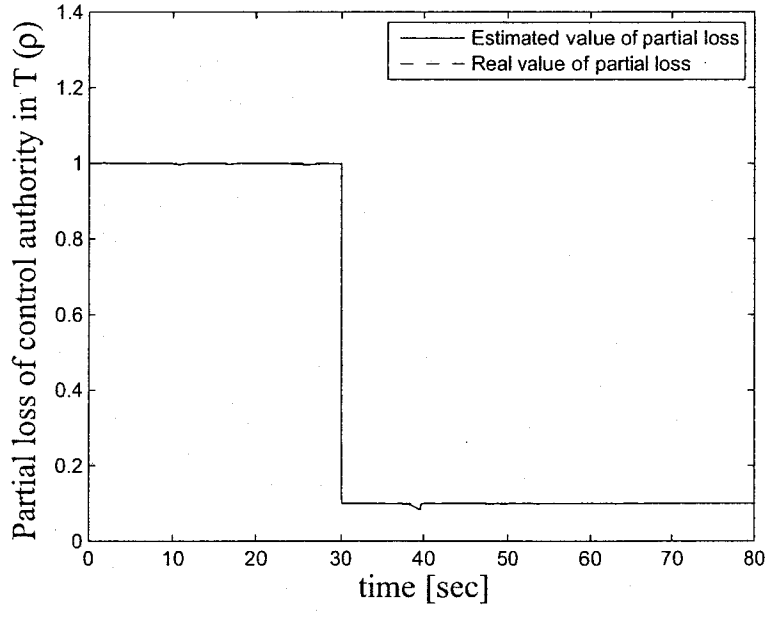

Figure 3.12: Fault identification in torque input T, $t_f = 30[sec]$ and $\rho = 0.1$

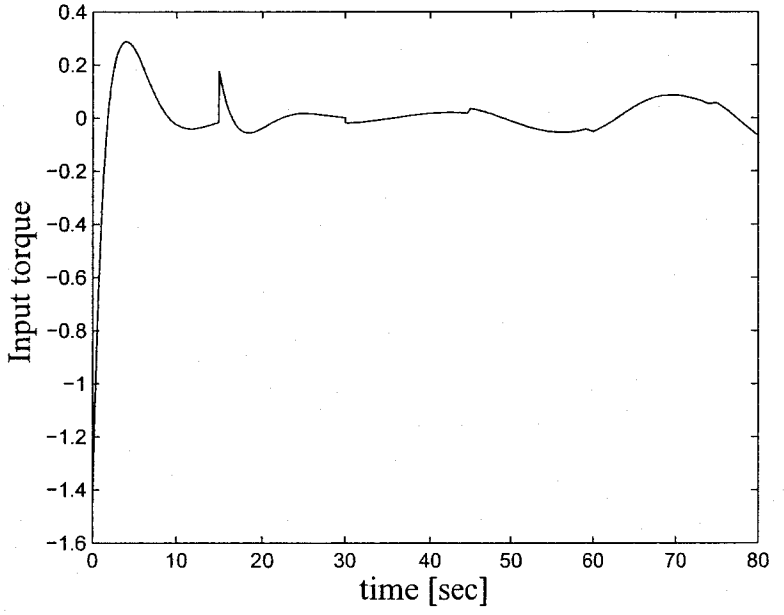

Figure 3.13: System input $t_f = 30[sec]$ and $\rho = 0.1$

zero value at a finite number of time instants, which is a set of measure zero. This shows that even for some cases where the input is zero at certain time instants the proposed methodology still works. This enables the observer to update the estimation of fault at all times. In the simulations shown in this chapter, the fault is always identified in less than $0.1[sec]$. It is observed that the proposed PWA fault identification method is capable of estimating the magnitude of the fault fast and accurately while the control input to the system is large enough for rapid updating of the estimated amount of fault.

3.4 Summary

In this chapter a fault identification technique for bimodal PWA systems is proposed. The proposed method enables to precisely estimate the unknown amount of the fault parameter based on a PWA representation of the system. The unknown value of the fault parameter is estimated by an adaptive law obtained from the Lyapunov function of the

system. Asymptotic stability of the fault estimation error is guaranteed provided the input norm is upper and lower bounded by positive constants. The proposed method is applied successfully to estimation of the amount of partial loss of control authority in a numerical example.

Chapter 4

An Active Fault-Tolerant Controller for Bimodal PWA Systems

4.1 Introduction

This chapter proposes a reconfigurable controller structure for bimodal PWA systems in order to increase reliability of the system. Fig. 4.1 shows schematic of the structure of the reconfigurable controller which is the interconnection of the fault identification observer proposed in chapter 3 and two sets of the fault-tolerant controllers of chapter 2, as a closed-loop system (CLS). The type of fault which is studied in this chapter is partial loss of control authority. In this chapter, loss of effectiveness faults are classified into two groups: severe faults and less severe faults. The controller design methodology proposed in chapter 2 is applied to design two sets of fault-tolerant controllers for the severe faults and less severe faults separately. Furthermore, the observer design methodology proposed in chapter 3, is applied to fault identification problem for bimodal PWA systems in this chapter. Once the fault is identified, the observer sends the estimated amount of fault to a controller switching mechanism. The controller switching mechanism decides which set

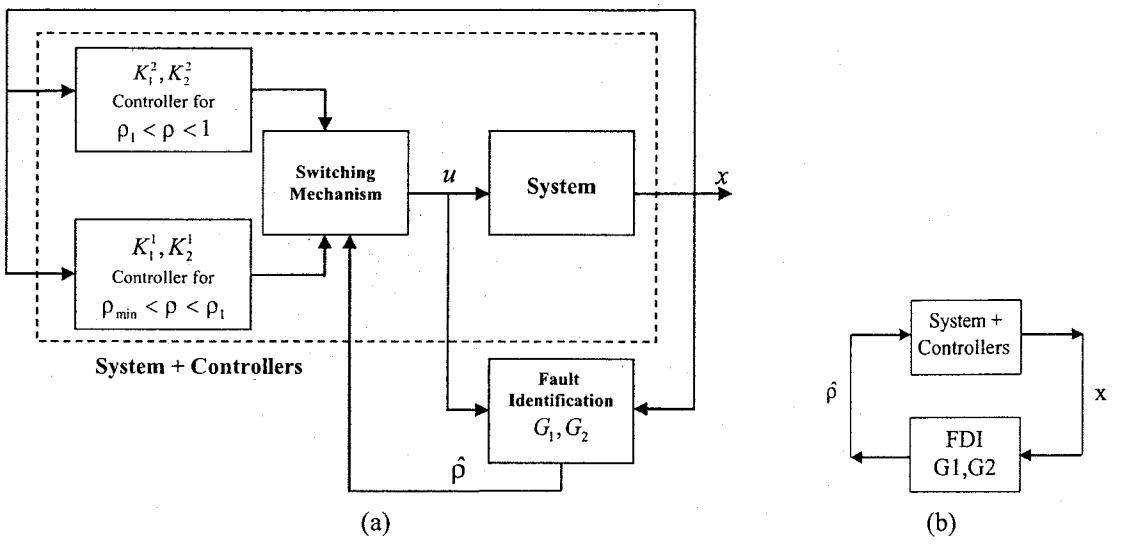

Figure 4.1: (a) Schematic of the CLS (b) The CLS viewed as a feedback interconnection

of the pre-designed fault-tolerant controllers must be in the loop, based on the identified amount of fault.

4.2 Active Fault-Tolerant Controller Synthesis

A bimodal PWA system of the following form is considered

$$\begin{cases} \dot{x}(t) = A_1 x(t) + B\rho u(t) & \forall x \in \mathscr{R}_1 \\ y(t) = C_1 x(t) \end{cases}$$

$$\begin{cases} \dot{x}(t) = A_2 x(t) + B\rho u(t) + m_2 & \forall x \in \mathscr{R}_2 \\ y(t) = C_2 x(t) \end{cases} \tag{4.1}$$

where $x(t) \in \mathbb{R}^n$ is the state vector and $u(t) \in \mathbb{R}^k$ is the input, $\mathscr{R}_1 \cup \mathscr{R}_2 = \mathscr{X}$ and

$$\mathscr{R}_2 = \{x \mid \| E_2 x + f_2 \| < 1\} \tag{4.2}$$

More precisely, if $\mathscr{R}_2 = \{x \mid d_1 < c_2^T x < d_2\}$, then the associated ellipsoidal covering is described by $E_2 = 2c_2^T/(d_2 - d_1)$ and $f_2 = -(d_2 + d_1)/(d_2 - d_1)$. The vector m_2 is

the affine term in region $\mathscr{R}_2$ which is a constant matrix. Without loss of generality, the dynamics in region $\mathscr{R}_1$, which contains the equilibrium point of the system, are considered to be linear. Therefore, $m_1 = \mathbf{0}$. The actual input might be reduced by a coefficient matrix ρ due to faults in the system where $\rho = diag\begin{bmatrix} 1 & \dots & \rho_i & \dots & 1 \end{bmatrix}$. The fault parameter ρ_i represents the unknown value of partial loss of control authority for only one actuator in the system where $\rho_i \in (0, 1]$. The structure of the observer is as follows,

$$\begin{cases} \dot{\hat{x}}(t) = A_1\hat{x}(t) + B\hat{\rho}(t)u(t) + G_1(\hat{y}(t) - y(t)) & \forall \hat{x} \in \mathscr{R}_1 \\ \hat{y}(t) = C_1\hat{x}(t) \end{cases}$$

$$\begin{cases} \dot{\hat{x}}(t) = A_2\hat{x}(t) + B\hat{\rho}(t)u(t) + m_2 + G_2(\hat{y}(t) - y(t)) & \forall \hat{x} \in \mathscr{R}_2 \\ \hat{y}(t) = C_2\hat{x}(t) \end{cases} \tag{4.3}$$

where $\hat{y}$, $\hat{\rho}$ and $\hat{x}$ are estimated variables. The fault parameter error is defined as $\tilde{\rho}(t) = \hat{\rho}(t) - \rho$. The estimation laws for the fault parameter have the following structure (for the i^{th} actuator where there is a fault)

$$\dot{\hat{\rho}}_i(t) = -l_i e^T(t) P b_i u_i(t) \tag{4.4}$$

where b_i is the i^{th} column of the B matrix. The error dynamics of the observer are presented in the equations (3.5), (3.6), (3.7), (3.8) in chapter 3.

Fault-tolerant controllers presented in chapter 2, are designed off-line for particular ranges of the fault values, including the nominal system for which $\rho_i = 1$. Since $\rho_i = 0$ represents total loss of control authority and is not addressed in this paper, we introduce ρ_{imin} which represents the most severe LOE fault in the i^{th} actuator and $\rho_{min} = diag\begin{bmatrix} 1 & \dots & \rho_{imin} & \dots & 1 \end{bmatrix}$. We also define ρ_{i1} as the average value of the fault range where $\rho_{i1} = \frac{\rho_{imin}+1}{2}$, separating less severe and most severe fault ranges, where $0 < \rho_{imin} <$

$\rho_{i1} < 1$ and $\rho_1 = diag\begin{bmatrix} 1 & \dots & \rho_{i1} & \dots & 1 \end{bmatrix}$. The state feedback control problem is parameterized by

$$u = K_j^1 x \qquad \forall\ \rho_{imin} \le \rho_i \le \rho_{i1} \quad \text{or} \tag{4.5a}$$

$$u = K_j^2 x \qquad \forall\ \rho_{i1} < \rho_i \le 1 \tag{4.5b}$$

where K_j^1 represents the controllers designed for the severe faults for $x \in \mathscr{R}_j$ and K_j^2 represents the controllers designed for less severe faults in region $\mathscr{R}_j$. The closed-loop system will be as follows

$$\forall \rho_{imin} \le \hat{\rho}_i \le \rho_{i1} \begin{cases} \dot{x}(t) = (A_1 + B\rho K_1^1)x(t) \quad \forall x \in \mathscr{R}_1 \\ y(t) = C_1 x(t) \end{cases} \\ \begin{cases} \dot{x}(t) = (A_2 + B\rho K_2^1)x(t) + m_2 \quad \forall x \in \mathscr{R}_2 \\ y(t) = C_2 x(t) \end{cases} \tag{4.6}$$

or

$$\forall \rho_{i1} < \hat{\rho}_i \le 1 \begin{cases} \dot{x}(t) = (A_1 + B\rho K_1^2)x(t) \quad \forall x \in \mathscr{R}_1 \\ y(t) = C_1 x(t) \end{cases} \\ \begin{cases} \dot{x}(t) = (A_2 + B\rho K_2^2)x(t) + m_2 \quad \forall x \in \mathscr{R}_2 \\ y(t) = C_2 x(t) \end{cases} \tag{4.7}$$

In the fault-tolerant controller design problem a performance criterion is added to the design. The cost function considered here is

$$J = \begin{cases} \int_0^\infty (\bar{x}^T \bar{\Upsilon} \bar{x} + u^T \Xi u) dt, \ \forall x \in \mathscr{R}_2 \\ \int_0^\infty (x^T \Upsilon x + u^T \Xi u) dt, \ \forall x \in \mathscr{R}_1 \end{cases} \tag{4.8}$$

where $\bar{x} = \begin{bmatrix} x \\ 1 \end{bmatrix}$, $x \in \mathbb{R}^n$ is the state vector of the system, $u = \bar{K}_j^i \bar{x}$, $\bar{K}_j^i = \begin{bmatrix} K_j^i & 0 \end{bmatrix}$, $\bar{\Upsilon} = \begin{bmatrix} \Upsilon & 0 \\ 0 & 0 \end{bmatrix}$, $\Upsilon \ge 0$ and $\Xi > 0$ are weighting matrices. The reconfigurable controller design problems are now presented.

Definition 4.2.1 Fault-Tolerant Controllers for Severe Faults *are the solution to the following optimization problem,* $K_j^1 = Y_j^1 Q_1, \forall x \in \mathscr{R}_j$ *where* $\hat{\rho}_i \in [\rho_{imin}, \rho_{i1}]$

$$\begin{aligned} \min \quad & \text{Trace}(P_1) \\ s.t. \quad & (4.9),\ (4.10) && \forall x \in \mathscr{R}_j \\ & (4.11),\ (4.12) && \forall x \in \mathscr{R}_{j0} \\ (4.13) \quad & Q_1 = Q_1^T > 0,\ \mu < 0, \end{aligned}$$

where (4.9), (4.10), (4.11), (4.12) and (4.13) are given by

$$\begin{bmatrix} \Gamma_2^1 + \mu m_2 m_2^T & Q_1 \Upsilon^{1/2} & {Y_2^1}^T \Xi^{1/2} & \mu m_2 f_2^T + Q_1 E_2^T \\ \Upsilon^{1/2} Q_1 & -I_n & 0 & 0 \\ \Xi^{1/2} Y_2^1 & 0 & -I_k & 0 \\ (\mu m_2 f_2^T + Q_1 E_2^T)^T & 0 & 0 & -\mu(1 - f_2 f_2^T) \end{bmatrix} < 0 \qquad (4.9)$$

where $\Gamma_2^1 = A_2 Q_1 + Q_1 A_2^T + B_f Y_2^1 + {Y_2^1}^T B_f^T$, $B_f = B\rho_1$ and $Y_2^1 = K_2^1 Q_1$.

$$\begin{bmatrix} \Gamma_{2f}^1 + \mu m_2 m_2^T & Q_1 \Upsilon^{1/2} & {Y_2^1}^T \Xi^{1/2} & \mu m_2 f_2^T + Q_1 E_2^T \\ \Upsilon^{1/2} Q_1 & -I_n & 0 & 0 \\ \Xi^{1/2} Y_2^1 & 0 & -I_k & 0 \\ (\mu m_2 f_2^T + Q_1 E_2^T)^T & 0 & 0 & -\mu(1 - f_2 f_2^T) \end{bmatrix} < 0 \qquad (4.10)$$

where $\Gamma_{2f}^1 = A_2 Q_1 + Q_1 A_2^T + B_{min} Y_2^1 + {Y_2^1}^T B_{min}^T$ and $B_{min} = B\rho_{min}$.

$$\begin{bmatrix} \Gamma_1^1 & Q_1 \Upsilon^{1/2} & {Y_1^1}^T \Xi^{1/2} \\ \Upsilon^{1/2} Q_1 & -I_n & 0 \\ \Xi^{1/2} Y_1^1 & 0 & -I_k \end{bmatrix} < 0 \qquad (4.11)$$

where $\Gamma_1^1 = A_1 Q_1 + Q_1 A_1^T + B_f Y_1^1 + {Y_1^1}^T B_f^T$ and $Y_1^1 = K_1^1 Q_1$.

$$\begin{bmatrix} \Gamma_{1f}^1 & Q_1\Upsilon^{1/2} & {Y_1^1}^T\Xi^{1/2} \\ \Upsilon^{1/2}Q_1 & -I_n & 0 \\ \Xi^{1/2}Y_1^1 & 0 & -I_k \end{bmatrix} < 0 \tag{4.12}$$

where $\Gamma_{1f}^1 = A_1Q_1 + Q_1A_1^T + B_{min}Y_1^1 + {Y_1^1}^T B_{min}^T$.

$$\begin{bmatrix} P_1 & I_n \\ I_n & Q_1 \end{bmatrix} > 0 \tag{4.13}$$

From the solution to this problem one gets the controller gains for severe fault $K_2^1 = Y_2^1Q_1$ and $K_1^1 = Y_1^1Q_1$.

Definition 4.2.2 Fault-Tolerant Controllers for Less Severe Faults *are the solution to the following optimization problem,* $K_j^2 = Y_j^2Q_2, \forall x \in \mathscr{R}_j$ *where* $\hat{\rho}_i \in (\rho_{i1}, 1]$

$$\begin{aligned} \min \quad & \text{Trace}(P_2) & \\ s.t. \quad & (4.14),\ (4.15) & \forall x \in \mathscr{R}_j \\ & (4.16),\ (4.17) & \forall x \in \mathscr{R}_{j0} \\ (4.18) \quad & Q_2 = Q_2^T > 0,\ \mu_2 < 0, & \end{aligned}$$

where (4.14), (4.15), (4.16), (4.17) and (4.18) are given by

$$\begin{bmatrix} \Gamma_2 + \mu_2 m_2 m_2^T & Q_2\Upsilon^{1/2} & {Y_2^2}^T\Xi^{1/2} & \mu_2 m_2 f_2^T + Q_2E_2^T \\ \Upsilon^{1/2}Q_2 & -I_n & 0 & 0 \\ \Xi^{1/2}Y_2^2 & 0 & -I_k & 0 \\ (\mu_2 m_2 f_2^T + Q_2E_2^T)^T & 0 & 0 & -\mu_2(1 - f_2f_2^T) \end{bmatrix} < 0 \tag{4.14}$$

where $\Gamma_2 = A_2Q_2 + Q_2A_2^T + BY_2^2 + {Y_2^2}^T B^T$ and $Y_2^2 = K_2^2Q_2$.

$$\begin{bmatrix} \Gamma_{2f}+\mu_2 m_2 m_2^T & Q_2\Upsilon^{1/2} & Y_2^{2T}\Xi^{1/2} & \mu_2 m_2 f_2^T + Q_2 E_2^T \\ \Upsilon^{1/2}Q_2 & -I_n & 0 & 0 \\ \Xi^{1/2}Y_2^2 & 0 & -I_k & 0 \\ (\mu_2 m_2 f_2^T + Q_2 E_2^T)^T & 0 & 0 & -\mu_2(1-f_2 f_2^T) \end{bmatrix} < 0 \tag{4.15}$$

where $\Gamma_{2f} = A_2 Q_2 + Q_2 A_2^T + B_f Y_2^2 + Y_2^{2T} B_f^T$ and $B_f = B\rho_1$.

$$\begin{bmatrix} \Gamma_1 & Q_2\Upsilon^{1/2} & Y_1^{2T}\Xi^{1/2} \\ \Upsilon^{1/2}Q_2 & -I_n & 0 \\ \Xi^{1/2}Y_1^2 & 0 & -I_k \end{bmatrix} < 0 \tag{4.16}$$

where $\Gamma_1 = A_1 Q_2 + Q_2 A_1^T + B Y_1^2 + Y_1^{2T} B^T$ and $Y_1^2 = K_1^2 Q_2$.

$$\begin{bmatrix} \Gamma_{1f} & Q_2\Upsilon^{1/2} & Y_1^{2T}\Xi^{1/2} \\ \Upsilon^{1/2}Q_2 & -I_n & 0 \\ \Xi^{1/2}Y_1^2 & 0 & -I_k \end{bmatrix} < 0 \tag{4.17}$$

where $\Gamma_{1f} = A_1 Q_2 + Q_2 A_1^T + B_f Y_1^2 + Y^{2T}_1 B_f^T$.

$$\begin{bmatrix} P_2 & I_n \\ I_n & Q_2 \end{bmatrix} > 0 \tag{4.18}$$

From the solution to this problem one gets the controller gains for less severe fault $K_2^2 = Y_2^2 Q_2$ and $K_1^2 = Y_1^2 Q_2$.

4.3 Application to a Wheeled Mobile Robot (WMR)

In this section, the proposed active fault-tolerant controller is applied to the same WMR model of chapter 3 with a new state space partitioning. The PWA models of the WMR for a regulation problem are

$\forall X \in \mathscr{R}_1$

$$\begin{bmatrix} \dot{x}_1 \\ \dot{x}_2 \\ \dot{x}_3 \end{bmatrix} = \begin{bmatrix} 0 & 1 & 0 \\ 0 & 0 & 1 \\ 0 & 0 & 0 \end{bmatrix} \begin{bmatrix} x_1 \\ x_2 \\ x_3 \end{bmatrix} + \begin{bmatrix} 0 \\ 0 \\ 1 \end{bmatrix} \rho u \tag{4.19}$$

$\forall X \in \mathscr{R}_2$

$$\begin{bmatrix} \dot{x}_1 \\ \dot{x}_2 \\ \dot{x}_3 \end{bmatrix} = \begin{bmatrix} 0 & 0.3729 & 0 \\ 0 & 0 & 1 \\ 0 & 0 & 0 \end{bmatrix} \begin{bmatrix} x_1 \\ x_2 \\ x_3 \end{bmatrix} + \begin{bmatrix} 0.4142 \\ 0 \\ 0 \end{bmatrix} + \begin{bmatrix} 0 \\ 0 \\ 1 \end{bmatrix} \rho u \tag{4.20}$$

where $X = \begin{bmatrix} x_1 & x_2 & x_3 \end{bmatrix}^T$. The state-space partitioning is

$$\begin{aligned} \mathscr{R}_1 &= \{X \in \mathbb{R}^3 \mid x_2 \in (-\frac{\pi}{4}, \frac{\pi}{4})\} \\ \mathscr{R}_2 &= \{X \in \mathbb{R}^3 \mid x_2 \in (\frac{\pi}{4}, \frac{\pi}{2})\} \end{aligned} \tag{4.21}$$

The ellipsoidal covering of the state-space partitioning is only defined for $\mathscr{R}_2$ where the system is affine

$$\varepsilon_2 = \{X \mid \| \begin{bmatrix} 0 & \frac{8}{\pi} & 0 \end{bmatrix} X - 3 \| < 1\} \tag{4.22}$$

In this example a path-following problem is addressed. Therefore, the tracking error is defined as $\delta(t) = X(t) - X_{des}$ where $X_{des} = \begin{bmatrix} y_{des} & 0 & 0 \end{bmatrix}^T$ and the rate of change of the tracking error as $\dot{\delta}(t) = \dot{X}(t) - \dot{X}_{des}$. Assume that $\dot{X}_{des} = 0$. Therefore, $\dot{\delta}(t) = \dot{X}(t)$.

$\forall \delta \in \mathscr{R}_1$

$$\begin{bmatrix} \dot{\delta}_1 \\ \dot{\delta}_2 \\ \dot{\delta}_3 \end{bmatrix} = \begin{bmatrix} 0 & 1 & 0 \\ 0 & 0 & 1 \\ 0 & 0 & 0 \end{bmatrix} \begin{bmatrix} \delta_1 \\ \delta_2 \\ \delta_3 \end{bmatrix} + \begin{bmatrix} 0 \\ 0 \\ 1 \end{bmatrix} \rho u \tag{4.23}$$

$\forall \delta \in \mathscr{R}_2$

$$\begin{bmatrix} \dot{\delta}_1 \\ \dot{\delta}_2 \\ \dot{\delta}_3 \end{bmatrix} = \begin{bmatrix} 0 & 0.3729 & 0 \\ 0 & 0 & 1 \\ 0 & 0 & 0 \end{bmatrix} \begin{bmatrix} \delta_1 \\ \delta_2 \\ \delta_3 \end{bmatrix} + \begin{bmatrix} 0.4142 \\ 0 \\ 0 \end{bmatrix} + \begin{bmatrix} 0 \\ 0 \\ 1 \end{bmatrix} \rho u \tag{4.24}$$

where $\delta = \begin{bmatrix} \delta_1 & \delta_2 & \delta_3 \end{bmatrix}^T = \begin{bmatrix} y - y_{des} & x_2 & x_3 \end{bmatrix}^T$. Please note that $x_2 = \delta_2$. Therefore, the switching, the state space partitioning and the ellipsoidal cells hold for the system of the path following problem.

A solution to the observer design problem in Theorem 1 is sought and obtained by SeDuMi/YALMIP [59] as

$$G_1 = \begin{bmatrix} -1257010.986811 & -0.333908 & -0.000002 \\ -0.333908 & -1254607.949079 & -0.506321 \\ -0.000002 & -0.506321 & -1254607.923042 \end{bmatrix} \tag{4.25}$$

$$G_2 = \begin{bmatrix} -1257139.052210 & 1301.965494 & -0.000345 \\ 1301.965494 & -1257331.495771 & -0.507120 \\ -0.000345 & -0.507120 & -1254958.817446 \end{bmatrix} \tag{4.26}$$

$$P = \begin{bmatrix} 4.0000 & 0.0000 & 0.0000 \\ 0.0000 & 4.0000 & 0.0000 \\ 0.0000 & 0.0000 & 4.0000 \end{bmatrix} \tag{4.27}$$

$$\lambda_2 = -1.1806, \quad \lambda_3 = -1.1847 \tag{4.28}$$

The reconfigurable controllers for severe faults $\rho_{min} \leq \hat{\rho} \leq \rho_1$ for $\rho_1 = 0.55$ and $\rho_{min} = 0.2$ are

$$K_1^1 = \begin{bmatrix} -1.1666 & -3.9598 & -6.3581 \end{bmatrix} \tag{4.29}$$

$$K_2^1 = \begin{bmatrix} -1.1945 & -3.8971 & -6.3916 \end{bmatrix} \tag{4.30}$$

The reconfigurable controllers for less severe faults $\rho_1 < \hat{\rho} \leq 1$ are

$$K_1^2 = \begin{bmatrix} -1.1308 & -3.0356 & -3.4246 \end{bmatrix} \tag{4.31}$$

$$K_2^2 = \begin{bmatrix} -1.2212 & -3.0164 & -3.4764 \end{bmatrix} \tag{4.32}$$

and

$$P_1 = \begin{bmatrix} 0.3854 & 0.3945 & 0.2206 \\ 0.3945 & 0.8324 & 0.5451 \\ 0.2206 & 0.5451 & 0.6312 \end{bmatrix} \times 10^{-3} \tag{4.33}$$

$$P_2 = \begin{bmatrix} 0.0005 & 0.0007 & 0.0006 \\ 0.0007 & 0.0020 & 0.0020 \\ 0.0006 & 0.0020 & 0.0032 \end{bmatrix} \tag{4.34}$$

For comparison purposes, an LQR controller is designed for the linear model of the system in (4.23). The weighting matrices for the LQR controller are

$$Q = \begin{bmatrix} 0.0001 & 0 & 0 \\ 0 & 0.0001 & 0 \\ 0 & 0 & 0.0001 \end{bmatrix}, R = 0.0001$$

The gains of the LQR controller are

$$K_{LQR} = \begin{bmatrix} 1.0000 & 2.4142 & 2.4142 \end{bmatrix} \tag{4.35}$$

Figs. 4.2-4.8 show the simulation results for the active fault-tolerant controller. In these simulations, a partial loss of control authority of 80% corresponding $\rho = 0.2$ occurs at $t_f = 30[sec]$. The path following capabilities of the proposed active fault-tolerant control method subject to a fault occurrence is compared to an LQR controller. Fig. 4.2 shows fault identification by the observer. Fig. 4.3 shows the input to the system versus

time. Fig. 4.4 shows the path of the WMR with the reconfigurable and the LQR controller. The switching sequence of the active fault-tolerant controller is shown in the Fig. 4.5. Fig. 4.6 shows the time response of y for the WMR. The observer gain in the loop for the WMR is shown in the Fig. 4.7. The time variation of the heading angle ψ of the WMR is shown in Fig. 4.8. It is observed that the LQR controller fails to follow the desired path. However, the reconfigurable controller stills follows the desired path with a good performance. Fig. 4.9 shows the comparison of the time responses of the system under the influence of the proposed active fault-tolerant controller in this chapter, the fault-tolerant controller proposed in chapter 2 and an LQR controller. In this figure, a partial loss of control authority of 80% corresponding $\rho = 0.2$ occurs at $t_f = 30[sec]$. It is observed that the time response of the system under the influence of the active fault-tolerant controller has a smaller overshoot and is faster compared to the time response of the system under the influence of the passive fault-tolerant controller proposed in chapter 2. Therefore, it is observed that the application of the active fault-tolerant controller improved the time response of the system.

4.4 Summary

This chapter proposes an active fault-tolerant controller structure for bimodal PWA systems. The proposed method is illustrated in a PWA model of a WMR. The path of the WMR is compared under the influence of both an LQR and the reconfigurable controller. It is observed that for severe faults, the LQR controller fails to follow the desired path while the active fault-tolerant controller follows the desired path.

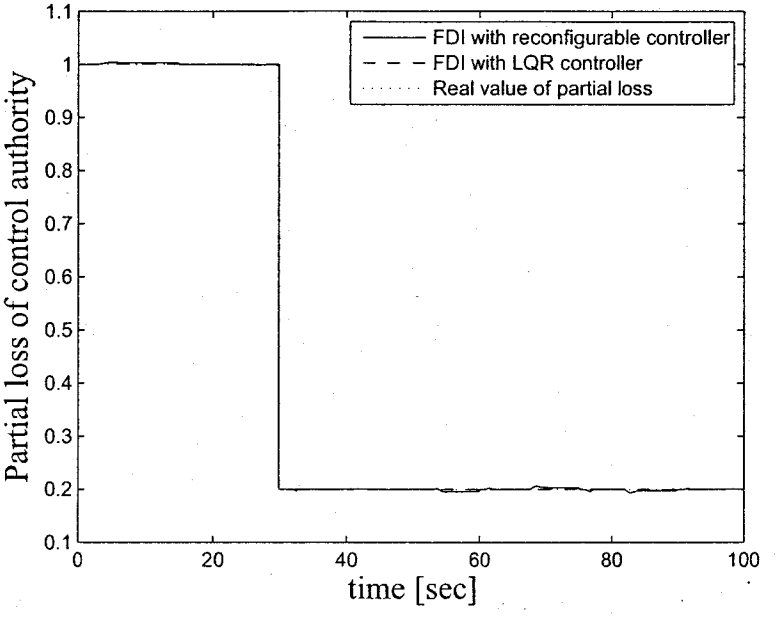

Figure 4.2: Fault identification, $t_f = 30[sec]$ and $\rho = 0.2$

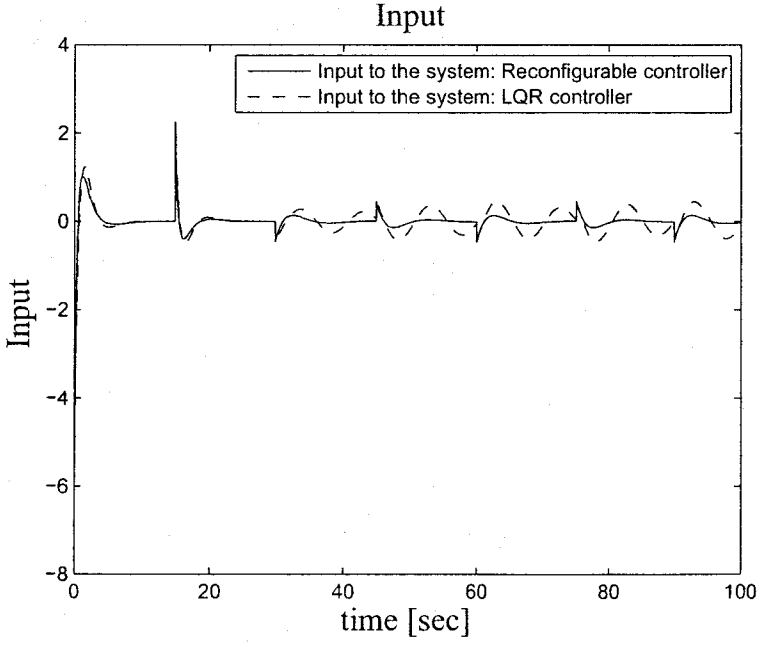

Figure 4.3: Input for $t_f = 30[sec]$ and $\rho = 0.2$

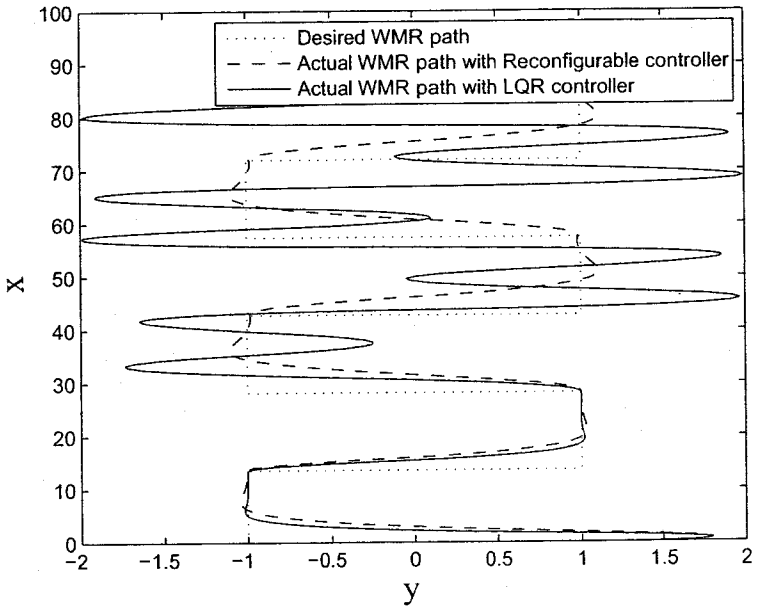

Figure 4.4: WMR path $t_f = 30[sec]$ and $\rho = 0.2$

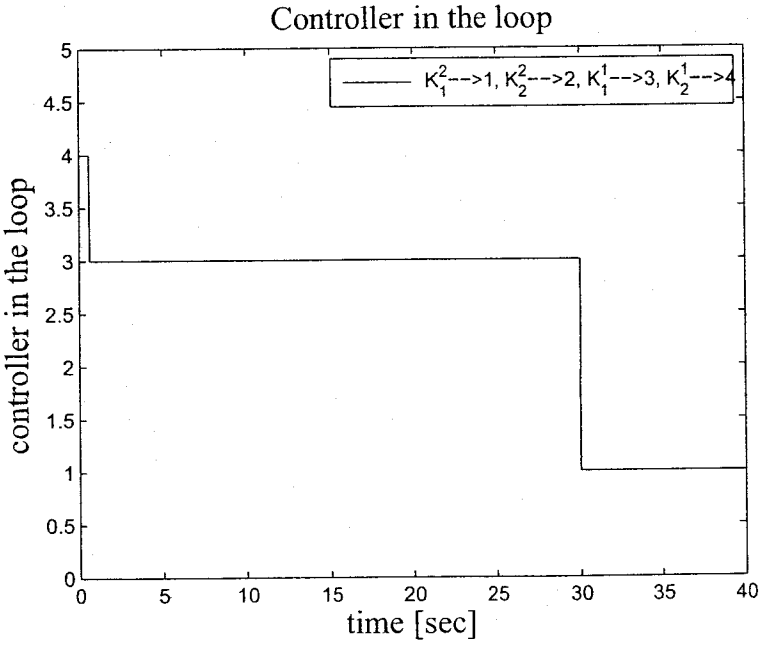

Figure 4.5: Controller switchings $t_f = 30[sec]$ and $\rho = 0.2$

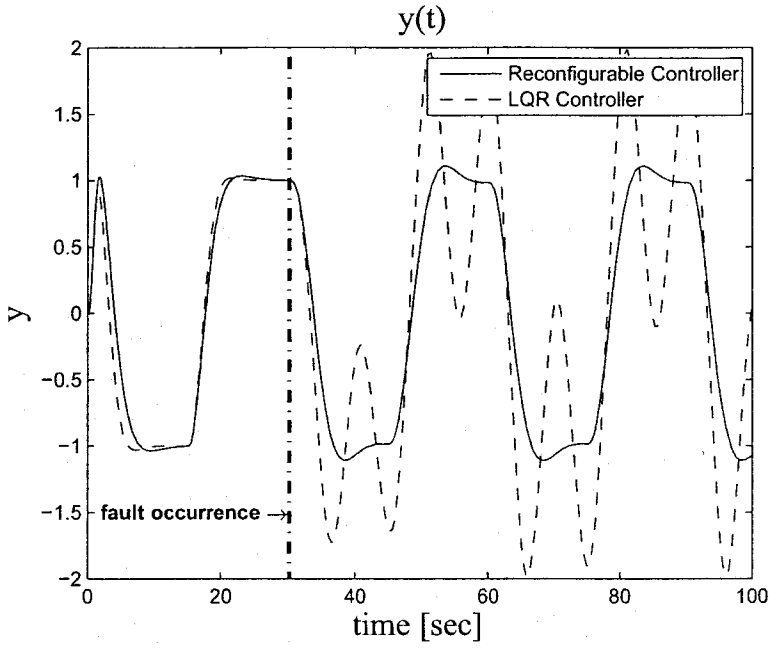

Figure 4.6: y(t), FTC and the LQR controller, $\rho = 0.2$

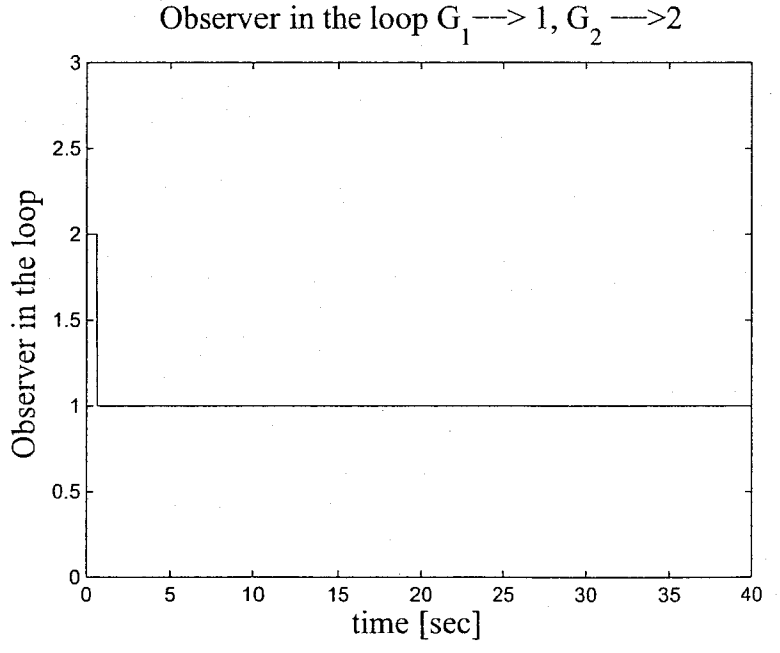

Figure 4.7: Observer in the loop $t_f = 30[sec]$ and $\rho = 0.2$

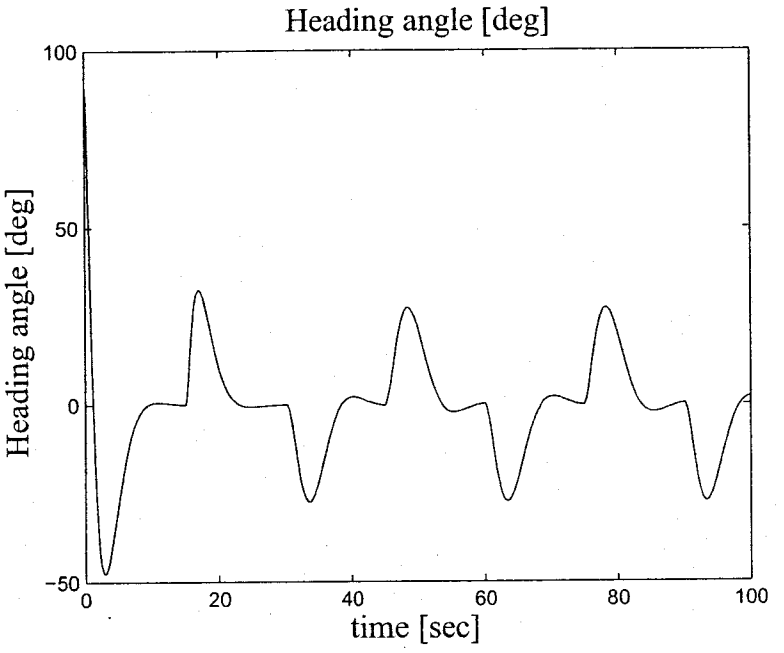

Figure 4.8: Heading angle ψ [deg], $t_f = 30[sec]$ and $\rho = 0.2$

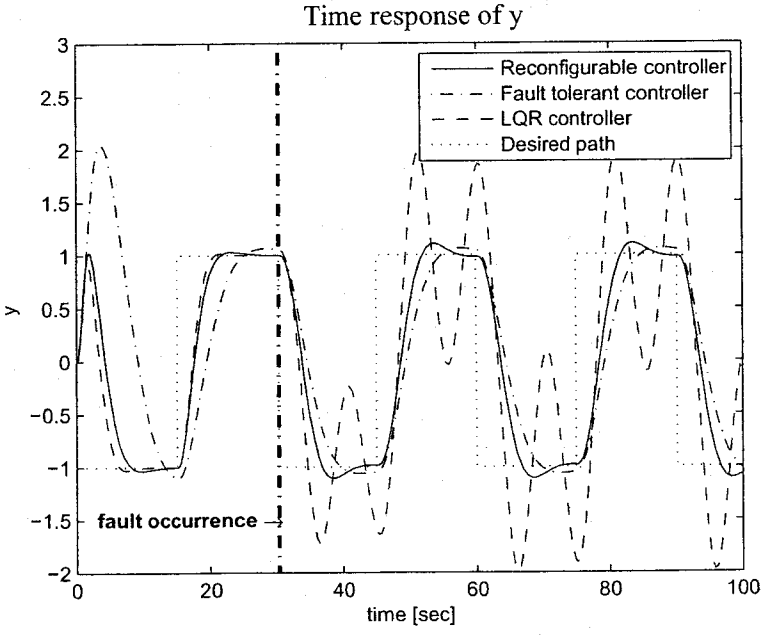

Figure 4.9: Active FTC, FTC and LQR controller,$\rho = 0.2$, $\psi_0 = \pi$, $y_0 = 0$

Chapter 5

Conclusions

In this chapter the contributions of the thesis are summarized and the conclusions from this research and potential future work are presented. In chapter 2, a fault-tolerant control design technique was introduced for PWA systems. The fault-tolerant controllers have inherent tolerance capability to LOE faults in the PWA system. The advantages of the proposed fault-tolerant controller design technique are that the proposed fault-tolerant controller is capable of stabilizing the nominal and faulty systems and that it provides a guaranteed cost performance for the nominal and fault systems. However, the drawback is that the fault-tolerant controller does not have any information about the existence and magnitude of a fault in the PWA system. The drawback was the motivation for the development of a fault identification mechanism for PWA systems in chapter 3 and further development of an active fault-tolerant controller proposed in Chapter 4. A few interesting extensions to the research work in chapter 2 would be the following

- to assume uncertainty in the dynamics of the system,
- to use an output feedback controller structure.

In chapter 3, a fault identification mechanism for bimodal PWA systems was introduced. The main advantage of the proposed fault identification mechanism is that it enables to precisely estimate the unknown amount of the fault parameter in the PWA system. The main drawback of the fault identification mechanism is the assumption that all the states are available for the observer. A few useful extensions to this work would be the following

- to assume that only some of the states of the system are available to the observers,
- to provide a logic for fault detection and isolation for PWA systems,
- to modify the observers so that they can detect, isolate and identify other types of faults such as lock-in-place and sensor faults,
- to consider multiple modes for the PWA system,
- to apply the proposed fault identification mechanisms to a complex example like an aircraft where there are several control input channels.

In order to modify the observer for identifying lock-in-place and sensor faults, one must design adaptive laws for the estimation of the affine term and the C matrix in the PWA system. An alternative structure for the adaptive law of the fault identification observer is

$$\dot{\tilde{\rho}}_i(t) = -l_i \varsigma_i \tilde{\rho}_i - l_i e^T(t) P b_i u_i(t)$$

which possibly results in an input-to-state stable observer. However, the alternative structure is not implementable. Therefore, an interesting future work would be to modify this structure for implementation.

In chapter 4, an active fault-tolerant controller structure for bimodal PWA systems was proposed. The fault-tolerant controllers proposed in chapter 2 and the fault identification mechanism proposed in chapter 3 were integrated in chapter 4 to form the active

fault-tolerant controller. The main advantage of the proposed active fault-tolerant controller is that it improves the performance of the system and actively responds to severe LOE faults. The main drawback is that faults are only allowed in one actuator of the system. The other drawback is that only two fault scenarios are considered: less severe faults and severe faults. Therefore, introducing more fault scenarios in the active fault-tolerant controller and allowing faults in all of the actuator channels could be subjects of future research work.

Bibliography

[1] H. Khalil, "Nonlinear Systems", *Prentice Hall*, 1996.

[2] D. Liberzon, D. Nesic, "Stability Analysis of Hybrid Systems Via Small-Gain Theorems", *Lecture Notes in Computer Science, Springer*, Vol. 3927, 2006, P: 421-435.

[3] Z.P. Jiang, A. R. Teel, L. Parly, "Small-Gain Theorem for ISS Systems and Applications", *Math. Control Signals Systems*, Vol. 7,1994, P: 95-120.

[4] E.D. Sontag, "On the Input-to-State Stability Property", *Systems and Control Letters*, Vol. 24, 1995, P: 351-359.

[5] E.D. Sontag, " Smooth Stabilization Implies Coprime Factorization", *IEEE Transactions on Automatic Control*, Vol. 34, 1989, P: 435-443.

[6] G. Zames, "On the Input-Output Stability of Time-varying Nonlinear Feedback Systems, Part 1: Conditions Derived Using Concepts of Loop Gain, Conicity and Positivity", *IEEE Transactions on Automatic Control*, Vol. 11, 1966, P: 228–238.

[7] A. Bacciotti, L. Mazzi, "An Invariance Principle for Nonlinear Switched Systems", *Systems and Control Letters*, Vol. 54, 2005, P: 1109-1119.

[8] J.P. Hespanha, "Uniform Stability of Switched Linear Systems: Extensions of LaSalles Invariance Principle", *IEEE Trans. Automat. Control*, Vol. 49, No. 4, 2004, P: 470-482.

[9] F. Mazenc, D. Nesic, "Strong Lyapunov Functions for Systems Satisfying the Conditions of LaSalle", *IEEE Trans. Automat. Control*, Vol. 49, No 6. , 2004, P: 1026–1030.

[10] K. Zhou, P. K. Rachinayani, N. Liu, Z. Ren and J. Aravena, "Fault Diagnosis and Reconfigurable Control for Flight Control Systems with Actuator Failures", *43rd IEEE Conference on Decision and Control*, Bahamas, December 2004, P: 5266-5271.

[11] N. E. Wu, Y. M. Zhang and K. Zhou, "Detection, Estimation, and Accommodation of Loss of Control Effectiveness", *International Journal of Adaptive Control and Signal Processing*, Vol. 14, No. 7, 2000, P: 775-795.

[12] Y. M. Zhang and J. Jiang, "An Active Fault-Tolerant Control System against Partial Actuator Failures", *IEE Proceedings Control Theory and Applications*, Vol. 149, No. 1, 2002, P: 95-104.

[13] Y. M. Zhang and X. R. Li, "Detection and Diagnosis of Sensor and Actuator Failures using IMM Estimator", *IEEE Transactions on Aerospace and Electronic Systems*, Vol. 34, No. 4, 1998, P: 1293-1313.

[14] Y. M. Zhang and J. Jiang, "Integrated Active Fault-Tolerant Control using IMM Approach", *IEEE Transactions on Aerospace and Electronic Systems*, Vol. 37, No. 4, 2001, P: 1221-1235.

[15] A. Jadbabaie, M. Jamshidi and A. Titli, "Guaranteed-Cost Design of Continuous-Time Takagi-Sugeno Fuzzy Controllers via Linear Matrix Inequalities", *IEEE World Congress on Computational Intelligence*, Fuzzy Systems Proceedings, Vol. 1, 1998, P: 268-273.

[16] D. J. Choi and P. Park, "Guaranteed Cost LPV Output-Feedback Controller Design for Nonlinear Systems", *Proceedings IEEE International Symposium on Industrial Electronics*, Vol. 2, 2001, P: 1198-1203.

[17] J.J.E. Slotine, W. Li, "Applied Nonlinear Control", *Englewood Cliffs, Prentice-Hall*, NJ, 1991.

[18] L. Rodrigues and E.-K. Boukas, "Piecewise-linear H_∞ Controller Synthesis with Applications to Inventory Control of Switched Production Systems," *Automatica*, Vol. 42, No. 8, 2006, P: 1245-1254.

[19] S. Shehab and L. Rodrigues, "UAV Path Following Using a Mixed Piecewise-Affine and Backstepping Control Approach," *European Control Conference*, Kos, Greece, 2007, P: 301-306.

[20] S. Casselman, L. Rodrigues, "A New Methodology for Piecewise Affine Models Using Voronoi Partitions", *48th IEEE conference on Decision and Control–CDC2009*, Shanghai, China, Dec. 16-18, 2009, P: 3920-3925.

[21] S. LeBel and L. Rodrigues, "Piecewise-Affine Parameter-Varying Control of Wheeled Mobile Robots" *American Control Conference*, Seattle, June 2008, P: 195-200.

[22] S. LeBel and L. Rodrigues, "PWL and PWA H_∞ Controller Synthesis for Uncertain PWA Slab Systems: LMI Approach", *International Journal of Control*, Vol. 82, No. 3, 2009, P: 482-492.

[23] B. Samadi and L. Rodrigues, "Extension of Local Linear Controllers to Global Piecewise Affine Controllers for Uncertain Nonlinear Systems", *International Journal of Systems Science*, Vol. 39 , No. 9, 2008, P: 867-879.

[24] N. Nayebpanah, L. Rodrigues and Y. M. Zhang, "Fault-Tolerant Controller Synthesis for Piecewise Affine Systems" *American Control Conference*, St. Louis, June 2009, P: 222-226.

[25] N. Nayebpanah, L. Rodrigues and Y. M. Zhang, "Fault Detection and Identification for Bimodal Piecewise Affine Systems", *American Control Conference*, St. Louis, June 2009, P: 2362-2366.

[26] W. P. M. H. Heemels, S. Weiland, " Input-to-State Stability and Interconnections of Discontinuous Dynamical Systems", *Automatica* , Vol. 44, No. 12, 2008, P: 3079-3086.

[27] W. P. M. H. Heemels, S. Weiland and A. Lj. Juloski, "Input-to-State Stability of Discontinuous Dynamical Systems with an Observer-Based Control Application", *Hybrid Systems: Computation and Control, Springer*, Vol. 4416, 2007, P: 259-272.

[28] L. Rodrigues and S. Boyd, "Piecewise-Affine State Feedback for Piecewise-Affine Slab Systems Using Convex Optimization", *Systems & Control Letters*, Vol. 54, No. 9, 2005, P: 835-853.

[29] L. Rodrigues, "State Feedback Control of Piecewise-Affine Systems with Norm Bounded Noise", *American Control Conference*, Portland, USA, June 2005, P: 1793-1798.

[30] D. Liberzon, "Switching in Systems and Control", *Volume in series Systems and Control, Birkhauser*, Boston, June 2003.

[31] A. Hassibi and S. Boyd, "Quadratic Stabilization and Control of Piecewise-Linear Systems", *American Control Conference*, Vol.6, June 1998, P: 3659-3664.

[32] W.P.M.H. Heemels, M. Lazar, N. van de Wouw, A. Pavlov, " Observer-based Control of Discrete-time Piecewise Affine Systems: Exploiting Continuity Twice", *47th IEEE Conference on Decision and Control, CDC 2008*, Cancun, Mexico, December 9-11, 2008, P: 4675-4680.

[33] M. Johansson, "Piecewise Linear Control System", *Lecture Notes in Control and Information Sciences*, Springer, 2003.

[34] M. Johansson, "Piecewise Linear Quadratic Optimal Control", *IEEE Transactions on Automatic Control*, Vol. 45, No. 4, 2000, P: 629-637.

[35] Y. M. Zhang and J. Jiang, "Bibliographical Review on Reconfigurable Fault-tolerant Control Systems", *Annual Reviews in Control*, Vol. 2, No. 2, 2008, P: 229-252.

[36] J. Jiang, "Fault-Tolerant Control Systems - An Introductory Overview", *Automatica SINCA*, Vol. 31, No. 1, 2005, P: 161-174.

[37] R. J. Patton, "Robustness Issues in Fault-Tolerant Control", *In Proceedings of the IEE Colloquium on Fault Diagnosis and Control System Reconfiguration*, 1993, P: 9/1-9/25.

[38] R. F. Stengel, "Intelligent Failure-Tolerant Control", *IEEE Control Systems Magazine*, Vol. 11, No. 4, 1991, P: 14-23.

[39] R. H. Miller, "Detection of the Loss of Elevator Effectiveness due to Aircraft Icing", *37th AIAA Aerospace Sciences Meeting and Exhibit*, Reno, NV, Jan. 11-14, 1999, AIAA-99-0637.

[40] P. E. Caines, "Lectures on Hybrid Control Systems", *McGill University*, 2009.

[41] `http://www.nasa.gov/centers/langley/news/factsheets/AvSP-factsheet.html`

[42] `http://www.dynamicflight.com/aerodynamics/loss_tail_eff`

[43] M. Ellison, "Optimal Linear Quadratic Control", *Lecture notes in Recursive Methods for Macroeconomics, The University of Warwick*, UK, 2004.

[44] Aircraft Icing Handbook, *Civil Aviation Authority*, 2000.

[45] P. R. Chandler,"Self-repairing Flight Control System Reliability and Maintainability ProgramExecutive Overview", *In Proceedings of the IEEE National Aerospace and Electronics Conference* , Dayton, OH, 1984, P: 586-590.

[46] J. S. Eterno, J. L. Weiss, D. P. Looze, A. S. Willsky, "Design Issues for Fault Tolerant-Restructurable Aircraft Control", *24th IEEE Conference on Decision and Control*, December, 1985, P: 900-905.

[47] A. Reehorst, J. Chung, M. Potapczuk, Y. Choo, W. Wright, T. Langhals, "An Experimental and Numerical Study of Icing Effects on the Performance and Controllability of a Twin Engine Aircraft", *NASA report*, January 1999.

[48] Aviation Education Multimedia Library, `http://www2.tech.purdue.edu/at/courses/aeml`

[49] X. Zhang, M. Polycarpou, T. Parisini. "A Robust Detection and Isolation Scheme for Abrupt and Incipient Faults in Nonlinear Systems", *IEEE Transactions on Automatic Control*, Vol. 47 , No. 4, 2002, P: 576-593.

[50] X. Zhang, T. Parisini, M. Polycarpou, "Adaptive Fault-Tolerant Control of Nonlinear Uncertain Systems: a Diagnostic Information-based Approach", *IEEE Transactions on Automatic Control*, Vol. 49, No. 8, 2004, P: 1259-1274.

[51] N. Meskin, K. Khorasani, "Actuator Fault Detection and Isolation for a Network of Unmanned Vehicles", *IEEE Transactions on Automatic Control*, Vol. 54 , No. 4, 2009, P: 835-840.

[52] D.Ye, G.-H. Yang, "Adaptive Fault-Tolerant Tracking Control Against Actuator Faults with Application to Flight Control", *IEEE Transactions on Control Systems Technology*, Vol. 14, No. 6, 2006, P: 1088-1096.

[53] D. Wang, K.Y. Lum, "Adaptive Unknown Input Observer Approach for Aircraft Actuator Fault Detection and Isolation" , *International Journal of Adaptive control and Signal Processing*, Vol. 21, 2007, P: 31-48.

[54] X. Zhang, M. M. Polycarpou, T. Parisini, "Design and Analysis of a Fault Isolation Scheme for a Class of Uncertain Nonlinear Systems", *Annual Reviews in Control*, Vol. 32, No. 1, 2008, P: 107-121.

[55] J.H. Richter, W.P.M.H. Heemels, N. van de Wouw and J. Lunze, "Reconfigurable Control of PWA Systems with Actuator and Sensor Faults: Stability", *47th IEEE Conference on Decision and Control*, Cancun, Mexico, 2008, P: 1060-1065.

[56] M. Rodrigues, D. Theilliol, D. Sauter, "Design of an Active Fault Tolerant Control and Polytopic Unknown Input Observer for Systems Described by a Multi-model Representation", *44th IEEE Conference on Decision and Control and the European Control Conference*, Seville, Spain, 2005, P: 3815- 3820.

[57] A.Lj. Juloski, W.P.M.H. Heemels, S. Weiland, "Observer Design for a Class of Piece-wise Affine Systems", *Proceedings of the 41st IEEE Conference on Decision and Control*, USA, 2002, P: 2606-2611.

[58] L. Rodrigues and J. How, "Observer-based Control of Piecewise-Affine Systems", *Proceedings of the 40th IEEE Conference on Decision and Control*, Orlando, FL, USA, 2001, P: 1366-1371.

[59] J. Lofberg, "YALMIP: A Toolbox for Modeling and Optimization in MATLAB", *In Proceedings of the CACSD Conference*, Taipei, Taiwan, 2004, P: 284-289.

[60] V. A. Jakubovic, "The S-procedure in Nonlinear Control Theory", *Vestnik Leningrad Univ. Math.* Vol. 4, 1977, P: 73-93.